(2000): Development of infantile rat ovaries autotransplanted after cryopreservation by vitrification. Theriogenology, 53,1093–1103.
14) Migishima, F., Suzuki-Migishima, R., Song, S.Y., Kuramochi, T., Azuma, S., Nishijima, M. and Yokoyama, M. (2003): Successful cryopreservation of mouse ovaries by vitrification. Biol. Reprod., 68, 881–887.
15) Chen, S.U., Chien, C.L., Wu, M.Y., Chen, T.H., Lai, S.M., Lin, C.W. and Yang, Y.S. (2006): Novel direct cover vitrification for cryopreservation of ovarian tissues increases follicle viability and pregnancy capability in mice. Hum. Reprod. 21, 2794–2800.
16) Wang, Y., Xiao, Z., Li, L., Fan, W. and Li, S.W. (2008): Novel needle immersed vitrification: a practical and convenient method with potential advantages in mouse and human ovarian tissue cryopreservation. Hum. Reprod., 23, 2256–2265.
17) Kasai, M. (1997): Vitrification: refined strategy for the cryopreservation of mammalian embryos. J. Mamm. Ova Res., 14, 17–28.
18) Martinez-Madrid, B., Dolmans, M.M., Langendonckt, A.V., Defrère, S., Van Eyck, A.S. and Donnez, J. (2004): Ficoll density gradient method for recovery of isolated human ovarian primordial follicles. Fertil. Steril., 82, 1648–1653.
19) Kyono. K., Fuchinoue, K., Yagi, A., Nakajo, Y., Yamashita, A. and Kumagai, S. (2005): Successful pregnancy and delivery after transfer of a single blastocyst derived from a vitrified mature human oocyte. Fertil. Steril., 84, 1017.
20) Huang, J.Y., Tulandi, T., Holzer, H., Tan, S.L. and Chian, R.C. (2008): Combining ovarian tissue cryobanking with retrieval of immature oocytes followed by in vitro maturation and vitrification: an additional strategy of fertility preservation. Fertil. Steril., 89, 567–572.
21) Telfer, E.E., McLaughlin, M., Dng, C. and Thong, K.J. (2008): A two-step serum-free culture system supports development of human oocytes from primordial follicles in the presence of activin. Hum. Reprod., 23, 1151–1158.
22) Dolmans, M.M., Donnez, J., Camboni, A., Demylle, D., Amorim, C., Van Langendonckt, A. and Prard, C. (2009): IVF outcome in patients with orthotopically transplanted ovarian tissue. Hum. Reprod., 24, 2778–2787.
23) Keros, V., Xella, S., Hultenby, K., Pettersson, K., Sheikhi, M., Volpe, A., Hreinsson, J. and Hovatta, O. (2009): Vitrification versus controlled-rate freezing in cryopreservation of human ovarian tissue. Hum. Reprod., 24, 1670–1683.
24) Yada-Hashimoto, N., Yamamoto, T., Kamiura, S., Seino, H., Ohira, H., Sawai, K., Kimura, T. and Saji, F. (2003): Metastatic ovarian tumors: a review of 64 cases. Gynecol. Oncol., 89, 314–317.
25) Donnez, J., Martinez-Madrid, B., Jadoul, P., Van Langendonckt, A., Demylle, D. and Dolmans, M.M. (2006): Ovarian tissue cryopreservation and transplantation: a review. Hum. Reprod. Update, 12, 519–535.
26) Martinez-Madrid, B., Camboni, A., Dolmans, M.M., Nottola, S., Van Langendonckt, A. and Donnez, J. (2007): Apoptosis and ultrastructural assessment after cryopreservation of whole human ovaries with their vascular pedicle. Fertil. Steril., 87, 1153–1165.
27) Schmidt, K.L., Andersen, C.Y., Loft, A., Byskov, A.G., Ernst, E. and Andersen, A.N. (2005): Follow-up of ovarian function post-chemotherapy following ovarian cryopreservation and transplantation. Hum. Reprod., 20, 3539–3546.
28) Anderson, R.A., Wallace, W.H. and Baird, D.T. (2008): Ovarian cryopreservation for fertility preservation: indications and outcomes. Reproduction, 136, 681–689.

In Vivo Safety and Persistence of Endoribonuclease Gene-Transduced CD4+ T Cells in Cynomolgus Macaques for HIV-1 Gene Therapy Model

Hideto Chono[1]*, Naoki Saito[1], Hiroshi Tsuda[1], Hiroaki Shibata[2], Naohide Ageyama[2], Keiji Terao[2], Yasuhiro Yasutomi[2], Junichi Mineno[1], Ikunoshin Kato[1]

1 Center for Cell and Gene Therapy, Takara Bio Inc, Otsu, Shiga, Japan, **2** Tsukuba Primate Research Center, National Institute of Biomedical Innovation, Tsukuba, Ibaraki, Japan

Abstract

Background: MazF is an endoribonuclease encoded by *Escherichia coli* that specifically cleaves the ACA sequence of mRNA. In our previous report, conditional expression of MazF in the HIV-1 LTR rendered CD4+ T lymphocytes resistant to HIV-1 replication. In this study, we examined the *in vivo* safety and persistence of MazF-transduced cynomolgus macaque CD4+ T cells infused into autologous monkeys.

Methodology/Principal Findings: The *in vivo* persistence of the gene-modified CD4+ T cells in the peripheral blood was monitored for more than half a year using quantitative real-time PCR and flow cytometry, followed by experimental autopsy in order to examine the safety and distribution pattern of the infused cells in several organs. Although the levels of the MazF-transduced CD4+ T cells gradually decreased in the peripheral blood, they were clearly detected throughout the experimental period. Moreover, the infused cells were detected in the distal lymphoid tissues, such as several lymph nodes and the spleen. Histopathological analyses of tissues revealed that there were no lesions related to the infused gene modified cells. Antibodies against MazF were not detected. These data suggest the safety and the low immunogenicity of MazF-transduced CD4+ T cells. Finally, gene modified cells harvested from the monkey more than half a year post-infusion suppressed the replication of SHIV 89.6P.

Conclusions/Significance: The long-term persistence, safety and continuous HIV replication resistance of the *mazF* gene-modified CD4+ T cells in the non-human primate model suggests that autologous transplantation of *mazF* gene-modified cells is an attractive strategy for HIV gene therapy.

Citation: Chono H, Saito N, Tsuda H, Shibata H, Ageyama N, et al. (2011) *In Vivo* Safety and Persistence of Endoribonuclease Gene-Transduced CD4+ T Cells in Cynomolgus Macaques for HIV-1 Gene Therapy Model. PLoS ONE 6(8): e23585. doi:10.1371/journal.pone.0023585

Editor: John J. Rossi, Beckman Research Institute of the City of Hope, United States of America

Received January 10, 2011; **Accepted** July 20, 2011; **Published** August 17, 2011

Funding: The authors have no support or funding to report.

Competing Interests: Hideto Chono, Naoki Saito, Hiroshi Tsuda, Junichi Mineno and Ikunoshin Kato are employees of Takara Bio Inc. (http://www.takara-bio.co.jp). There are no patents, products in development or marketed products to declare. This does not alter the authors' adherence to all the PLoS ONE policies on sharing data and materials.

* E-mail: chonoh@takara-bio.co.jp

Introduction

Highly active anti-retroviral therapy (HAART) is widely used for human immunodeficiency virus (HIV) therapy and involves the combination of several drugs with different functions that are currently being evaluated in clinical trials; some of these drugs are currently available [1]. HAART treatment reduces plasma viral load to undetectable levels and recovers CD4+ T cells to clinically safe levels. Although HAART therapy has revolutionized the treatment of HIV-1 infection, the need for life-long therapy, difficulties with medication adherence and long-term medication toxicities have led to the search for new treatment strategies that will efficiently reduce the viral load and allow for stable immunological homeostasis. The number of patients who are HAART resistant has significantly decreased in the past 2 years due to newly available drugs, but based on previous experience, drug resistance is likely to increase again. Thus, additional approaches for the management of HIV infection, or approaches performed in combination with HAART therapy, are needed. Gene therapy for HIV-1 infection has been proposed as an alternative to antiretroviral drug regimens [2,3]. A number of different genetic vectors with antiviral payloads have been utilized to combat HIV-1, including antisense RNA against the HIV-1 envelope gene, transdominant protein RevM10, ribozymes, RNA decoys, single chain antibodies, and RNA-interference [4,5]. These protocols use T cells or hematopoietic stem cells as a target for gene modification. Autologous T cell transfer in HIV patients began in the mid 1990's, and since that time, no serious adverse events have been reported to be associated with infusions of autologous T cells, and infusions are well tolerated. The majority of these clinical trials used gene transfer by retrovirus or lentiviral vectors for the delivery of the anti-HIV payloads.

In order to develop a new approach for HIV therapy, we previously constructed an HIV-1 Tat-dependent expression retroviral vector in which the *Escherichia coli* (*E. coli*) endoribonuclease gene *mazF* was fused downstream of the trans-activation

response element (TAR) so that the gene expression of *mazF* is induced upon HIV-1 replication [6]. When MazF-transduced cells were infected with HIV-1 IIIB, the replication of HIV-1 was efficiently inhibited without affecting CD4+ T cell growth. MazF-transduced primary CD4+ T cells derived from monkeys also suppressed simian/human immunodeficiency virus (SHIV) replication [6]. Thus, autologous transfer of genetically modified CD4+ T cells conditionally expressing the MazF protein will be a promising strategy for HIV gene therapy. Generally, the shift from the chronic phase to the AIDS phase is due to the balance between viral growth and immune suppression, and the remarkable decrease in CD4+ T cells causes the subsequent deficiency of the immune system, the hallmarks of AIDS. The benefit of the MazF-based gene therapy strategy is that gene-modified CD4+ T cells may be protected from HIV-1-associated cell death and are therefore likely to help the immune system maintain a stable condition.

In this preclinical study, we examined the *in vivo* safety and persistence of MazF-transduced autologous CD4+ T cells (named MazF-Tmac cells) using a non-human primate model. Cynomolgus macaque primary CD4+ T cells were retrovirally transduced with the MazF vector, infused into the autologous monkeys, and the persistence and safety of the MazF-Tmac cells was monitored more than half a year. We found that infused MazF-Tmac cells were detected in the peripheral blood throughout the experimental period. Additionally, experimental autopsy revealed the distribution of the infused lymphocyte in total body.

Results

Manufacturing of MazF-transduced CD4+ T cells using *ex vivo*-expanded cynomolgus macaque CD4+ T cells

In order to infuse more than 1×10^9 MazF-transduced autologous cells, isolated primary CD4+ T lymphocytes were *ex vivo* stimulated, transduced with the MT-MFR-PL2 retroviral vector (Figure 1A), and expanded as described in the Materials and Methods. The resultant MazF-Tmac cells were transplanted into autologous monkeys via intravenous infusion (Figure 1B). We initially used concanavalin A (Con A) for the stimulation of CD4+ T cells (CD4T-1), but Con A only induced a 12-fold cell expansion after 7 days. In order to improve the *ex vivo* expansion, we used anti-CD3/anti-CD28 monoclonal antibody-conjugated beads (anti-CD3/CD28 beads), which are known to yield a more efficient cellular expansion [7,8]. As we expected, the fold expansion of CD4+ T cells (CD4T-2 and CD4T-3) stimulated with anti-CD3/CD28 beads was much higher than with Con A stimulation (Table 1). In order to improve the engraftment efficiency of CD4+ T cells, busulfan was orally administered to the macaques prior to the transplantation, and the gene-modified MazF-Tmac cells were infused into each monkey intravenously at $1.6–2.7\times10^9$ cells.

Transduction efficiency and cell surface markers of MazF-Tmac cells

The efficiency of MazF transduction and phenotype of cell surface markers of the MazF-Tmac cells were analyzed using flow cytometry. The MazF vector transduction efficiency of CD4T-2 and CD4T-3 cells was 61.8% and 60.0%, respectively, while only 34.5% for CD4T-1 (Table 1). As shown in Table 2, 99% of the expanded MazF-Tmac cells were CD3 and CD4 double-positive, and in these cells, more than 90% expressed CD95/CD28, which are known central memory phenotype markers [9]. Central memory cells generally have a longer life span compared to effecter memory cells [10]; thus, a higher percentage of central memory cells in MazF-Tmac cells is likely to result in longer persistence after transplantation. Furthermore, to assess the activation status of MazF-Tmac cells, we measured the expression of CD25, which is also known as IL-2 receptor alpha and is an activated T cell marker. CD25 expression of MazF-Tmac cells from CD4T-2 and CD4T-3 was low. In contrast, almost 100% of the CD4+ T cells were found to express CD25 with a higher expression level 2–4 days after stimulation (data not shown). Thus, these data indicate that a large number of MazF-Tmac cells entered into resting or non-activated states during the *ex vivo* culture. CXCR4, a co-receptor for X4 tropic HIV entry, was found to be expressed in expanded CD4T-2 and CD4T-3 MazF-Tmac cells. Furthermore, we observed that there was no significant difference in the measured cell surface markers between Con A- and anti-CD3/CD28 bead-stimulated MazF-Tmac cells (Table 2).

Longitudinal analysis of infused MazF-Tmac cells

To examine the *in vivo* safety and persistence of infused MazF-Tmac cells, peripheral blood from each monkey was collected to monitor the hematological effects and the proviral copy number of the transduced retroviral vector in the genome over six months. There was no significant change in the body weight of the monkeys throughout the experiment (Figure 2A). During the period of 2–4 weeks post-transplantation, severe reduction in the white blood cell (WBC) count, hemoglobin (Hb) concentration, and platelet (PLT) levels were observed in the monkeys CD4T-1 and CD4T-2, while only slight reduction was observed in CD4T-3. These negative effects are considered to be due to the effect of the busulfan treatment, which is known to cause partial bone marrow depletion and functional defects in blood-forming tissues. No other adverse events were observed throughout the experiments. The transient reduction of lymphocytes gradually recovered, and the cell number became stable two months after the transplantation (Figure 2A).

The percentage of persistent MazF-Tmac cells in CD4+ T cells was determined using real-time PCR and flow cytometric analyses. The percentage of MazF-Tmac cells gradually decreased in CD4T-1- and CD4T-2-transplanted monkeys, while in the CD4T-3-transplanted monkey, a drastic reduction of the infused MazF-Tmac cells was observed 3–4 weeks post-transplantation but was not observed at later time points (Figure 2B). Although the levels of MazF-Tmac cells gradually decreased over time, the infused MazF-Tmac cells were detected even after six months post-transplantation. It is reasonable to assume that a population of infused MazF-Tmac cells can persist for a long-term period, likely forming a resting condition.

Detection of anti-MazF antibodies in monkey blood

Although the levels of MazF-transduced CD4+ T cells gradually decreased in the peripheral blood, some were detected throughout the half-year experimental period, suggesting that MazF-Tmac cells showed little or no immunogenicity towards cynomolgus macaques. Because gene therapy for HIV is aimed at reconstituting an HIV-resistant immune system, genetically modified cells must not only inhibit virus replication, but also maintain their expected trafficking behavior and persist *in vivo*. Although the evidence of longitudinal persistence of MazF-Tmac cells supports the low immunogenicity of MazF-Tmac cells, it is important to assess the production of antibodies against MazF. As shown in Figure 3 and Figure S1, we detected no production of anti-MazF antibodies in the CD4T-2 monkey blood after transplantation of the MazF-Tmac cells.

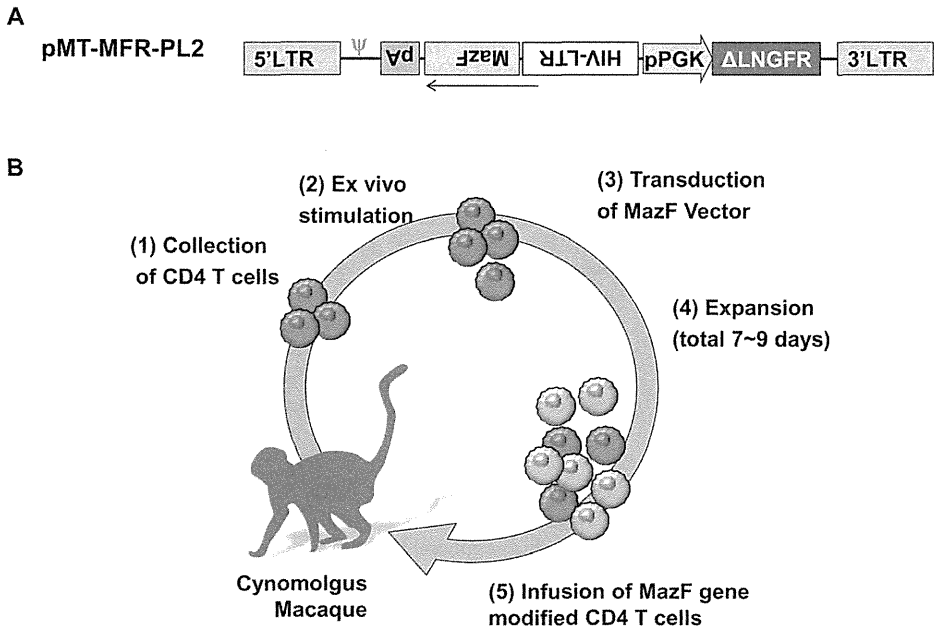

Figure 1. Diagram of autologous CD4+ T cell transplantation using a non-human primate model. (A) Design of gene transfer vector. The MazF gene derived from *E. coli* was inserted directly into the downstream of HIV-LTR sequence. The HIV-LTR-MazF-polyA cassette was introduced in the opposite direction of the MoMLV-LTR. A truncated form of the human ΔLNGFR was also introduced into the retrovirus vector as a surface marker. The ΔLNGFR gene is under the control of the human PGK promoter. (B) Flow diagram of gene-transduced CD4+ T cell manufacture. (1) Peripheral blood was collected by apheresis, (2) CD4+ T cells were selected by positive selection and stimulated *ex vivo* with Con A or anti-CD3/CD28 monoclonal antibody-conjugated beads. (3) The MT-MFR-PL2 vector was transduced twice on days 3 and 4. (4) The transduced cells were expanded for an additional 3–5 days until the total cell number reached more than 10^9. (5) On day 7–9, the expanded cells were collected, washed, and infused to the autologous macaques through venous blood.
doi:10.1371/journal.pone.0023585.g001

In vivo safety of MazF-Tmac cells

It is a great advantage to use primate models for investigating the safety of gene-modified cells, as they can be used for surgical pathological analysis. Therefore, we performed experimental autopsies six months after transplantation. To examine the safety of MazF-Tmac cells, specimens from several organs were fixed in buffered formaldehyde and embedded in plastic. Serial sections were made using a diamond saw. Slides were then stained with hematoxylin-eosin. Histopathological findings of the specimens were contracted with Bozo Research Center (Tokyo, Japan), and no severe adverse events relating to MazF-Tmac cell infusion was observed (Table 3 and Figure S2).

Table 1. Demographic data and summary of expansion fold and transduction efficiency.

	CD4T-1	CD4T-2	CD4T-3
Body Weight (kg)	5.25	5.18	3.7
Method for stimulation	Con A	Anti-CD3/CD28 Beads	Anti-CD3/CD28 Beads
Number of stimulated CD4+ T cells ($\times 10^7$ cells)	13.0	1.0	4.6
Days for expansion (days)	7	7	9
Number of infused MazF-Tmac cells ($\times 10^9$ cells)	1.6	1.7	2.7
Expansion Fold	12.3	170	58.7
Gene transfer efficiency (%)	34.5	61.8	60.0

doi:10.1371/journal.pone.0023585.t001

Examination of the anti-viral efficacy of MazF-Tmac cells harvested from monkey

In order to examine whether the Tat-dependent expression of MazF and anti-viral efficacy was maintained in the MazF-Tmac cells after infusion, CD4+ T lymphoid cells from a CD4T-1-transplanted monkey (214 days post-infusion of MazF-Tmac cells) were selected and expanded *ex vivo* (Figure 4A). After 7 days of expansion, the genetically modified cells expressing a truncated form of the human low affinity nerve growth factor (ΔLNGFR+) were concentrated with an anti-CD271 monoclonal antibody (Figure 4B). CD271-positive cells and CD271-negative cells were expanded for an additional 4 days. Both groups of expanded cells were infected with SHIV 89.6P [11] at the multiplicity of infection (MOI) of 0.01. Culture supernatants and cell pellets were analyzed at 6 days post-infection. As shown in Figure 4C, the replication of SHIV 89.6P was significantly suppressed in CD271-positive cells

Table 2. Cell surface markers of expanded MazF-Tmac cells.

	CD4T-1	CD4T-2	CD4T-3
CD3(+)/CD4(+) (%)	98.2	98.7	99.9
CD95(−)/CD28(+) (Naïve) (%)	0.7	1.2	0.4
CD95(+)/CD28(+) (CM) (%)	93.0	94.7	91.2
CD95(+)/CD28(−) (EM) (%)	6.2	3.9	8.3
CXCR4 (%)	N/A	92.0	79.4
CD25 (%)	N/A	30.4	24.5

CM: Central Memory, EM: Effector Memory.
doi:10.1371/journal.pone.0023585.t002

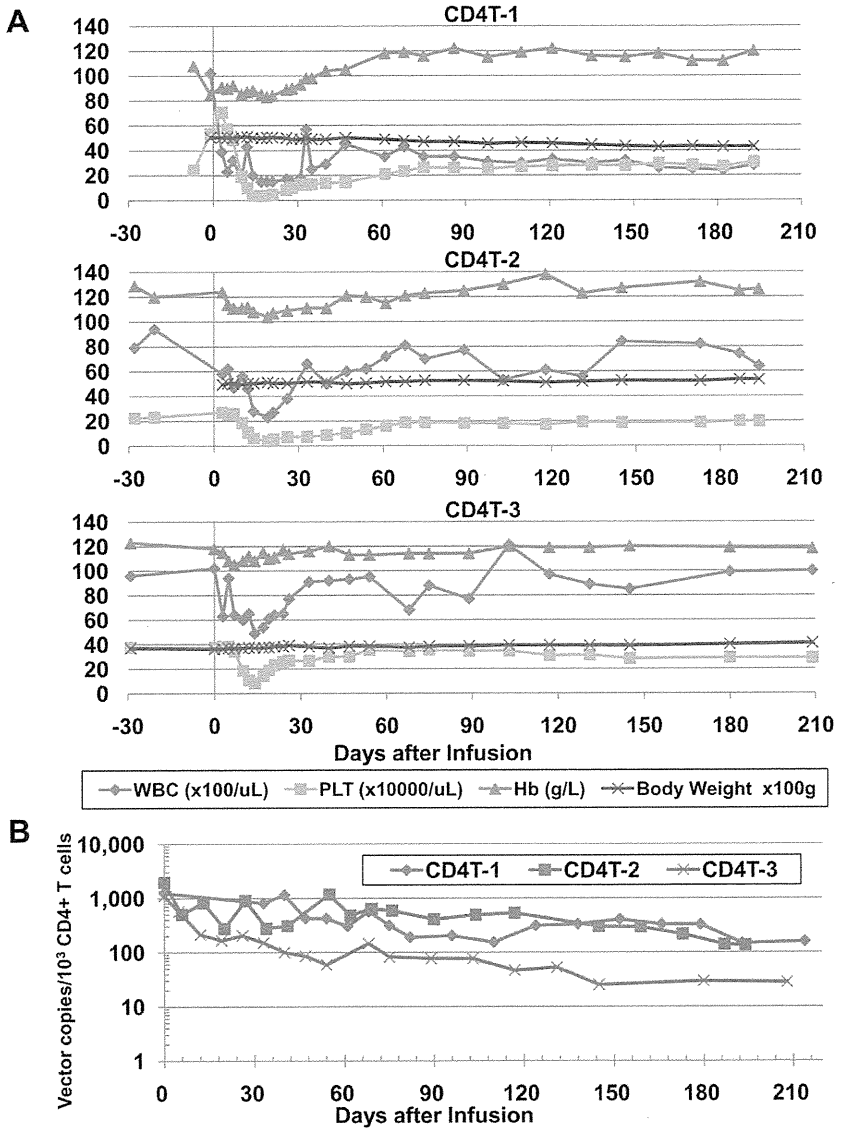

Figure 2. Hematological analysis and engraftment of the MazF-transduced CD4+ T cells. (A) The body weight and several hematological features were measured at the indicated time points, and the number of WBC, Hb, and PLT were represented. Each macaque was monitored throughout the study period. (B) The *in vivo* persistence of retroviral-transduced CD4+ T cells in the peripheral blood. PBMCs were collected at the indicated time points. The percentage of CD4+ T cells was analyzed using flow cytometry, and the proviral MazF vector copy was analyzed using real-time PCR. By compounding these two data, the copy number of the *mazF* gene in CD4+ T cells was calculated.
doi:10.1371/journal.pone.0023585.g002

in comparison with CD271-negative cells. Although western blot analysis managed to detect the expression of MazF, MazF was below the detection limit (data not shown). However, the expression of MazF was clearly induced when the same CD271-positive cells were transduced with the Tat expression retroviral vector M-LTR-Tat-ZG [6] (Figure 4D). These data suggest that the conditional expression system in MazF-Tmac cells is still active at 6 months post-transplantation.

Distribution of MazF-Tmac cells

To examine the distribution and persistence of the infused MazF-Tmac cells in a monkey, lymphocytes isolated from several organs were analyzed using flow cytometry and real-time PCR. As shown in Figure 5A and 5B, ΔLNGFR+ cells were detected in CD4+ T cells isolated from several lymph nodes (LNs), spleen, and peripheral blood. A similar tendency was obtained using real-time PCR (Figure 5C). In contrast, MazF-Tmac cells were not detected in the bone marrow, liver, thymus, and small intestine (data not shown). These data strongly suggest that infused MazF-Tmac cells mainly circulate in the secondary lymphoid organs.

In vivo distribution of MazF-Tmac cells treated with or without retinoic acid

Based on the findings that MazF-Tmac cells were well distributed among secondary lymphoid organs but not in small intestine, we performed additional experiment using one cynomolgus monkey (CD4T-4). In order to investigate the editing effect of the homing receptor to efficiently recruit the gene-modified cells to intestinal tissues in a non-human primate model, the distribution of retinoic acid-treated MazF-Tmac cells was

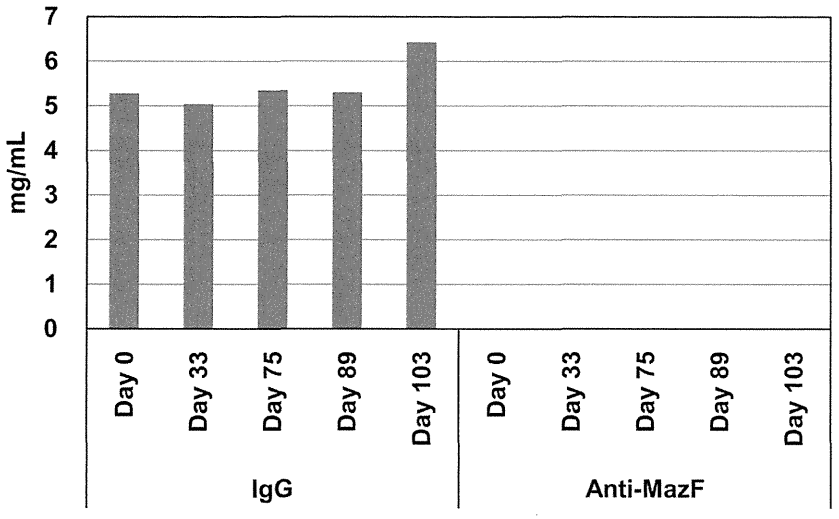

Figure 3. No detection of anti-MazF antibodies in monkey blood after transplantation of MazF-Tmac cells. Plasma samples were isolated from the monkey CD4T-2 at day 0, 33, 75, and 103 after transplantation and were used to detect anti-MazF antibodies on a MazF protein-immobilized microplate. The plasma samples were diluted to 500,000-fold, 50,000-fold, and 10,000-fold and added to each well. After the incubation, antibodies which reacted with immobilized MazF were tried to detect as described in Materials and Methods. No MazF-specific antibodies were detected.
doi:10.1371/journal.pone.0023585.g003

examined in a cynomolgus macaque. The experimental procedure is described in Figure 6A. Non-treated and retinoic acid-treated MazF-Tmac cells were designated as MazF-Tmac-N and MazF-Tmac-R, respectively. Expressions of integrin-α4 and integrin-β7 were remarkably increased in the presence of retinoic acid (Figure 6B). Thereafter, MazF-Tmac-N and MazF-Tmac-R were labeled with carboxyfluorescein diacetate succinimidyl ester (CFSE) and PKH26, respectively. The CFSE-labeled cells were mixed with an equal number of PKH26-labeled cells (Figure 6C), and 6.8×10^8 of the mixed cells were infused into a CD4T-4 monkey. Note that the transduction efficiency of the MazF vector was 65% (data not shown). Three days after the transplantation, experimental autopsy was performed to obtain samples of several organs as described in the Materials and Methods. Both the CFSE- and the PKH26-labeled CD4+ T cells were detected in the peripheral blood and several LNs by FACS analysis (Figure 6D). The percentage of the infused cells in the LNs was low compared to the peripheral blood, indicating that a large number of the infused cells did not migrate to the secondary lymphoid tissues and circulated in the peripheral blood at this time point. In the case of the inguinal and axillary LNs, the percentage of MazF-Tmac-R cells was low compared to MazF-Tmac-N cells. In contrast, a higher percentage of MazF-Tmac-R cells was observed in the mesenteric LN compared to MazF-Tmac-N cells. MazF-Tmac-N cells were evenly distributed in the three LNs analyzed, while the MazF-Tmac-R cells seemed to be preferentially distributed in the mesenteric LNs. Moreover, a large number of MazF-Tmac-R cells were distributed in the small intestine, while MazF-Tmac-N cells were not. To further evaluate the homing effect of the MazF-Tmac cells, the distribution of the labeled-MazF-Tmac cells in cryopreserved organs was analyzed using fluorescence microscopy (Figure 6E). A number of the PKH26-labeled MazF-Tmac-R cells were observed in the mesenteric LNs and in Peyer's patches. Taken together, retinoic acid-treated MazF-Tmac cells seem to be selectively recruited to mesenteric LNs and then transported to Peyer's patches. The distribution of MazF-Tmac-R cells in the intestinal villi remains to be determined.

Table 3. Analysis of *in vivo* safety (Histological finding about autopsy sample).

	CD4T-1	CD4T-2	CD4T-3
Lymph node	±	±	–
Spleen	–	–	±
Bone marrow	++**	–	–
Thymus	N/A	+*	–
Small intestine	–	–	–
Liver	–	–	–
Kidney	–	±	–
Pancreas	–	–	–
Stomach	–	–	±
Lung	–	±	–
Heart	–	–	±

–: No remarkable changes; ±: Minimal; +: Mild; ++: Moderate.
N/A: No equivalent sample available.
*Due to the Aging,
**Side effect due to the busulfan administration.
doi:10.1371/journal.pone.0023585.t003

Discussion

MazF is a toxin encoded by the *E. coli* genome and plays a role in growth regulation under stress conditions in *E. coli* [12]. MazF can act as an endoribonuclease (RNase) that specifically cleaves cellular mRNAs at ACA sequences [13]. Therefore, MazF induction in *E. coli* virtually eliminates almost all cellular mRNAs to completely inhibit protein synthesis. However, MazF-induced cells retain full capacity for protein synthesis, as MazF-induced cells are able to produce a protein at a high level if the prerequisite mRNA is engineered to be devoid of all ACA sequences without altering its amino acid sequence [14]. This indicates that RNA components involved in protein synthesis are protected from

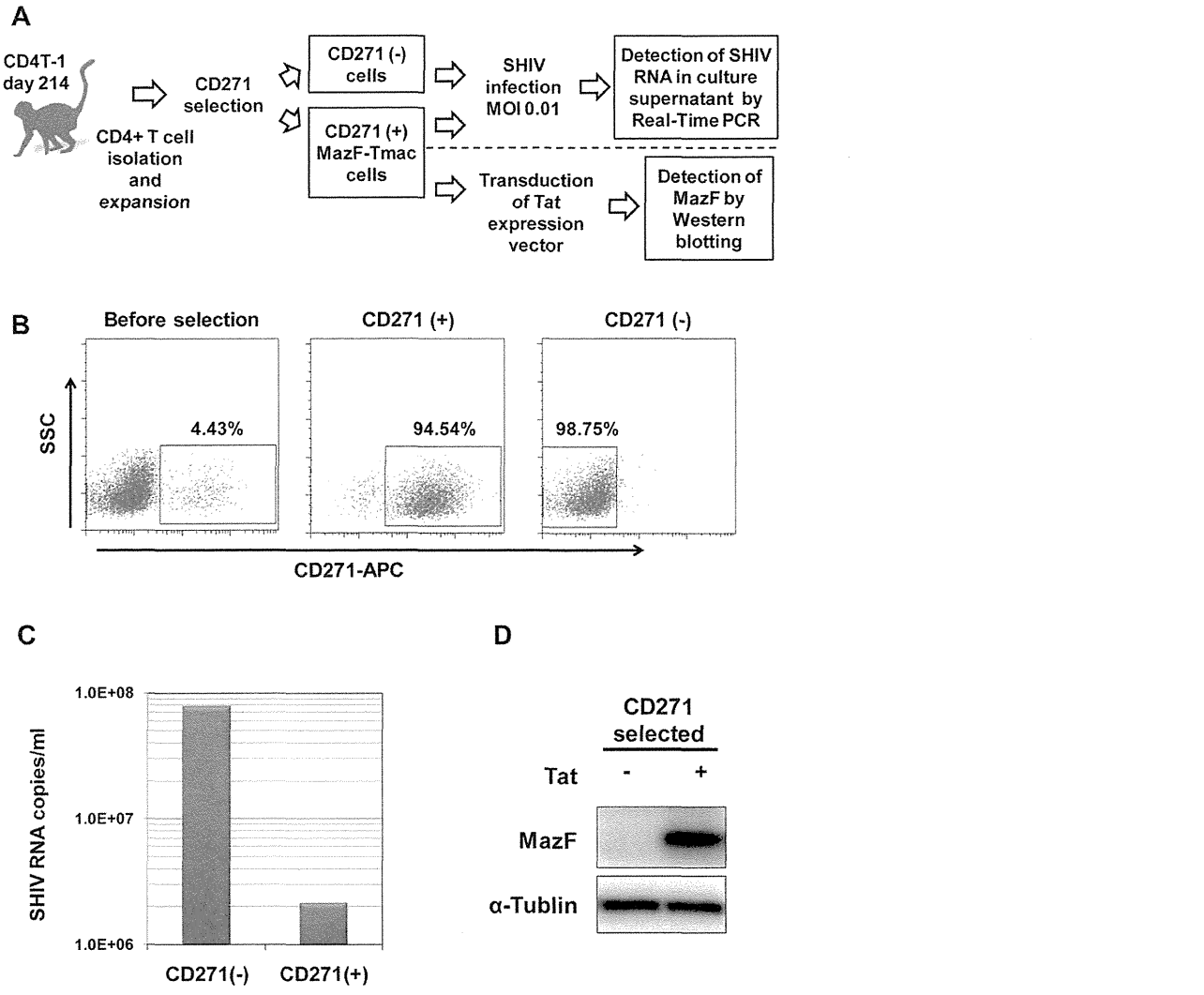

Figure 4. Examination of the anti-viral efficacy of MazF-Tmac cells harvested from the monkey. (A) Flow diagram of the experiment. CD4+ T lymphoid cells from CD4T-1 (214 days post-infusion of the MazF-Tmac cells) were stimulated and expanded *ex vivo*. The genetically modified cells expressing ΔLNGFR+ were concentrated with an anti-CD271 monoclonal antibody and expanded for 4 days. The expanded CD271-enriched cells and CD271-negative cells were infected with SHIV 89.6P. SHIV RNA levels in the culture supernatant were determined using quantitative real-time PCR. Expression of MazF was detected from the cell lysates by western blot analysis. Moreover, CD271-positive cells were transduced with the Tat expression vector. (B) CD271-positive and -negative cells were enriched using an anti-CD271 antibody, and dot plots of the flow cytometry analysis are presented. (C) The suppression of SHIV RNA in the culture supernatant at 6 days after infection was detected by real-time PCR analysis. (D) MazF-Tmac cells transduced with the Tat expression vector were harvested at 20 hours post-transduction and used for western blot analysis. Conditional expression of MazF in a Tat-dependent manner was observed.
doi:10.1371/journal.pone.0023585.g004

MazF cleavage. Indeed, ribosomal RNAs (rRNAs) and transfer RNAs (tRNAs) are protected from MazF cleavage in *E. coli* [15].

RNase-based anti-HIV gene therapy is an attractive strategy to suppress HIV-1 RNA replication. In the case of MazF, there are more than 240 ACA sequences in HIV-1 RNA, suggesting that HIV has almost no chance to gain MazF-related escape mutations. This approach seems to have a substantial advantage over the other known antiviral strategies, including antiviral drug therapy, and RNA-based gene therapies, such as antisense RNA, ribozyme, and siRNA.

MazF overexpressed in mammalian cells preferentially cleaves messenger RNAs (mRNAs), but not ribosomal RNAs [16]. As HIV-1 RNA has more than 240 ACA sequences, we assumed that the viral RNA is highly susceptible to MazF, leading to inhibition of viral replication under a conditional expression system. Indeed, conditional expression of MazF with Tat suppresses replication of both HIV-1 IIIB and SHIV 89.6P without affecting cellular mRNAs, suggesting that this Tat-dependent expression system of MazF is an attractive payload for HIV gene therapy [6]. It is an intriguing phenomenon that viral RNAs are efficiently and preferentially cleaved without affecting cellular mRNAs, and we are now addressing this question. Meanwhile, MazF is a bacterial protein, and its expression is induced by Tat protein; thus, it is important to assess the safety and immunogenicity of *mazF* gene-modified cells *in vivo*. In order to determine the safety of our MazF-retrovirus system *in vivo*, we infused MazF-transduced CD4+ T cells into cynomolgus macaques. In human gene therapy trials, engraftment of 1–2% of genetically modified cells in the peripheral

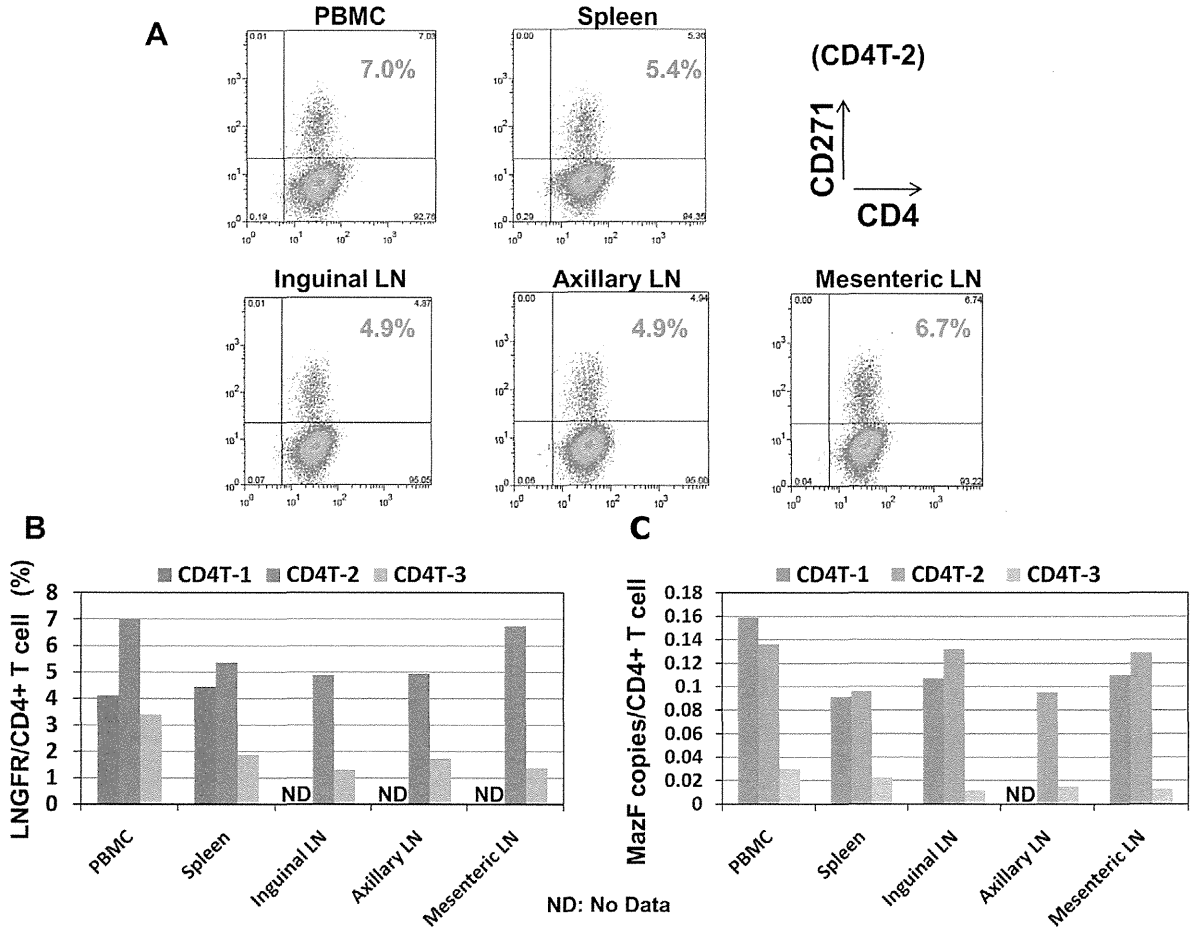

Figure 5. Analysis of the distribution of MazF-Tmac cells in several organs. (A) CD4+ T cells were isolated from lymphocytes separated from several organs, incubated 3–4 days, and stained with anti-CD4 and anti-CD271 antibodies. CD4T-2 is represented by a dot plot. (B) The percentage of CD271+ cells from three macaques is summarized. (C) The Copy number of the MazF gene in CD4+ T cells from each organ was calculated from real-time PCR and flow cytometric data.
doi:10.1371/journal.pone.0023585.g005

circulation has been observed following infusions of about 10 billion cells [17], and higher cell doses results in higher levels of engraftment [18,19]. Infusions of lower than 5×10^9 cells do not reliably result in measurable engraftment levels [19]. Therefore, we decided to infuse more than one billion cells into cynomolgus macaques, reflecting one-tenth of the scale of the human model. Indeed, the *mazF* gene-modified cells were detected over a six month period at a high level, and no histopathological disorders and no MazF-specific antibody production was observed during the experiment, demonstrating that MazF-Tmac cells showed little or no immunogenicity to monkeys. Moreover, MazF-Tmac cells harvested from the CD4T-1-transplanted monkey 6 months post-infusion showed resistance to the replication of SHIV 89.6P, indicating that the long-term persistent MazF-Tmac cells are functional. The expression of MazF in the SHIV-infected MazF-Tmac cells was below the limit of detection due to a low MOI such as 0.01, while in the MazF-Tmac cells transduced with the Tat expression retroviral vector M-LTR-Tat-ZG at 45% efficiency, expression of MazF was clearly induced, indicating that Tat dependent MazF expression system was maintained in the cells even 6 months after the autologous transplantation.

Because gene therapy for HIV is aimed at reconstituting an HIV-resistant immune system, genetically modified cells must inhibit virus replication and maintain persistence *in vivo*. Although *ex vivo* gene therapy targeting CD4+ T cells or CD34+ hematopoietic stem cells has been shown to promote long term persistence of infused cells in peripheral blood in human, it is difficult to obtain information about the distribution pattern of these cells in the whole human body. In order to obtain such information, the monkeys were sacrificed and lymphocytes were isolated from several organs after 6 months of monitoring. Importantly, the infused MazF-Tmac cells were detected in secondary lymphoid tissue, such as several LNs and spleen, and in peripheral blood, although individual differences between CD4T-1, -2, and -3-transplanted monkeys were observed. No histopathological disorders were observed in the organs containing MazF-Tmac cells, indicating that there were no lesions relating to MazF-Tmac cells. The distribution of MazF-Tmac cells in the lymphoid tissues of CD4T-3-transplanted monkey was lower compared to the CD4T-1 and -2-transplanted monkeys. One reason for this phenomenon is likely the lower dosage of busulfan used to treat the CD4T-3-transplated monkey. Busulfan is an alkylating agent with potent effects on hematopoietic stem cells that is commonly used for stem cell transplantation. In rhesus macaques, a low-dose of busulfan has an impact on bone marrow stem/progenitor cells with transient and mild suppression of peripheral blood counts

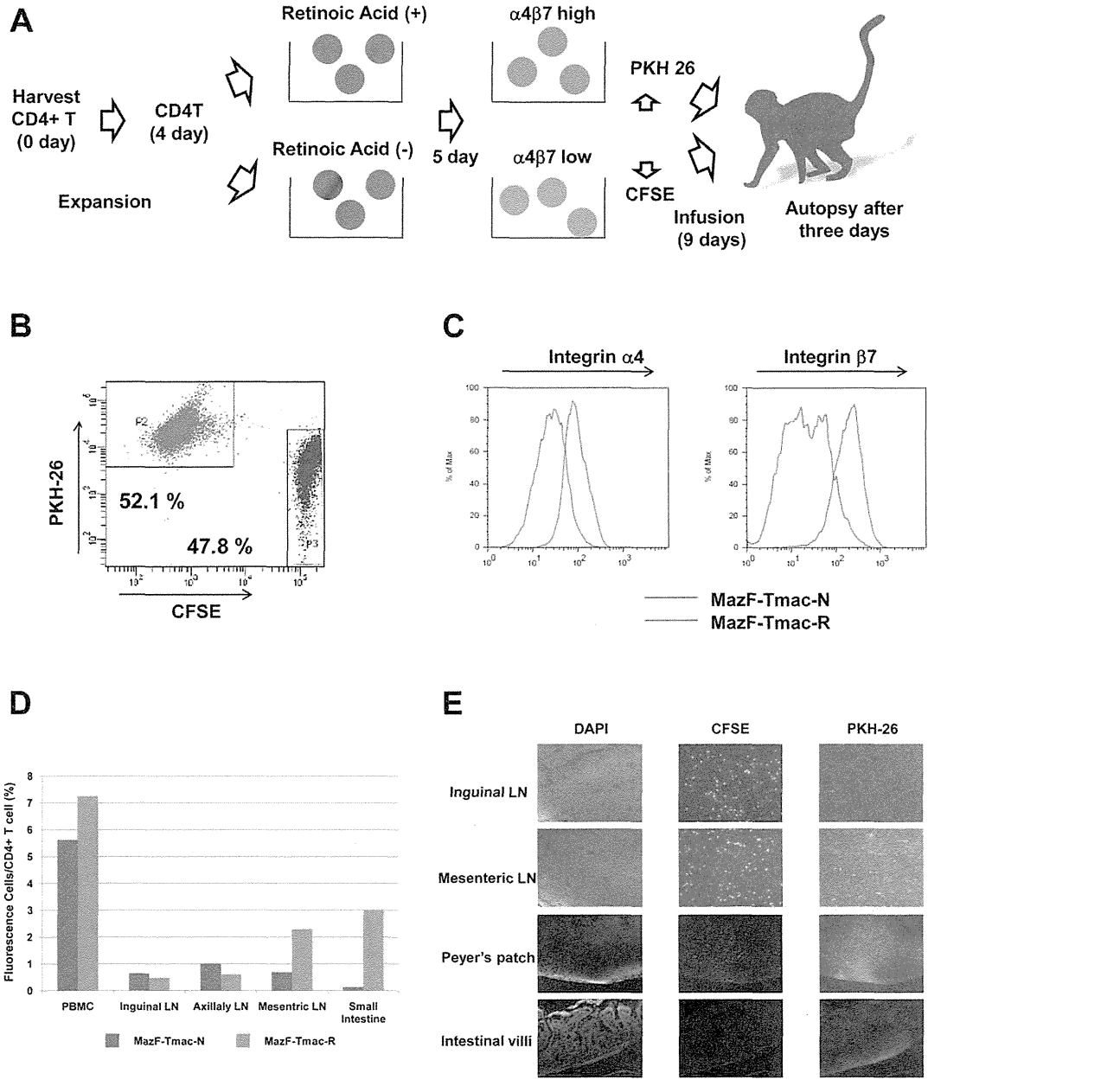

Figure 6. Comparison of the homing effect of MazF-Tmac cells treated with or without retinoic acid. (A) CD4+ T cells from the CD4T-4 monkey were stimulated with anti-CD3/CD28 beads, and MT-MFR-PL2 vector was transduced twice on days 3 and 4. After transduction, total lymphocytes were divided into two culture conditions in which retinoic acid was added to the one. After an additional 5 days of incubation, control and retinoic acid-treated cells were stained with CFSE and PKH26, respectively, mixed at nearly the same numbers, and infused into the autologous CD4T-4. Three days after the transplantation, experimental autopsy was performed. (B) A mixture of the two groups of MazF-Tmac cells stained with CFSE and PKH26 was analyzed using flow cytometry; the ratio of the two groups was almost same. (C) Up-regulation of the homing receptor was confirmed in the MazF-Tmac-R cells. The MazF-Tmac-N and MazF-Tmac-R cells are indicated by the blue line and red line, respectively. (D) Lymphocytes were collected from three lymph nodes (LNs) and small intestines, and a percentage of fluorescently-labeled cells were analyzed by flow cytometry. (E) Fluorescence microscope analysis of distal organ specimens.
doi:10.1371/journal.pone.0023585.g006

[20]. Thus, the lower engraftment efficiency of CD4T-3 (MazF-Tmac) cells might be due to the milder busulfan treatment.

In contrast to the LNs and spleen, a limited number of cells were detected in non-lymphoid tissues such as small intestine and liver. Considering HIV-1 infection, the gastrointestinal (GI) tract, which contains the vast majority of lymphoid tissues in the total body to protect mucosal membranes from foreign antigens, is the dominant site of HIV replication rather than LNs, which were originally thought to be the main infection sites [21]. In GI tract, CD4+ T cells are dramatically decreased during the acute phase of HIV infection [21,22,23]. In rhesus macaques, a similar depletion was also reported during the acute phase of simian immunodeficiency virus (SIV) infection, with CD4+ memory T cells specifically targeted [24,25]. Notably, the rate of mucosal CD4+

T cell depletion in pathogenic SIV-infected monkeys correlates with the disease progression in the rhesus macaque [26]. Indeed, recent studies provide evidence that the depletion of mucosal CD4+ T cells leads to damage of the gut mucosal layer resulting in translocation of microbial products, such as lipopolysaccharide (LPS), ultimately causing chronic and systemic immune activation, which is one of the hallmarks of HIV/SIV infection and one of the predictors of disease progression [27,28]. Although HAART therapy is effective in controlling viral replication and recovering CD4+ T cells in the peripheral blood, restoration of CD4+ T cells is delayed in the GI tract [21,29]. Thus, the repair of depleted CD4+ T cells using gene therapy might attenuate the breakdown of the mucosal layer and prevent mucosal immune system deficiency. To change the tissue distribution of infused CD4+ T cells, the enhancement of homing receptor expression in T lymphocyte is necessary. Integrin $\alpha4\beta7$ is known to facilitate the migration of lymphocytes from gut-inductive sites where immune responses are first induced (Peyer's patches and mesenteric LNs) to the lamina propria [30,31]. Expression of the homing receptor is induced by the addition of retinoic acid [32], which is produced mainly from retinol (vitamin A) by dendritic cells in the mesenteric LNs. As shown in Figure 6D and 6E, although these are preliminary data with only one monkey, editing of the homing receptors integrin-$\alpha4$ and integrin-$\beta7$ by retinoic acid enhanced the recruitment of MazF-Tmac cells to the mesenteric LNs, small intestine, and Peyer's patches. These results may indicate that MazF-Tmac cells treated with retinoic acid selectively accumulate in the mesenteric LNs and then migrate into Peyer's patches. It has been reported that the HIV-1 envelope protein gp120 binds to and signals through the activated form of integrin $\alpha4\beta7$ [33]; however, we expect that retinoic acid-treated MazF-T cells will persist in distal organs without the additional spread of HIV replication because of the HIV-1 resistance observed in the MazF-Tmac cells. Therefore, we speculate that the combination of several culture methods to edit the homing receptor will enhance the recruitment of MazF-Tmac cells to distal lymphoid organs, resulting in a more efficient therapeutic.

In summary, we showed long-term persistence, safety and continuous HIV replication resistance in the *mazF* gene-modified CD4+ T cells in a non-human primate model *in vivo*, suggesting that autologous transplantation of *mazF* gene-modified cells is an attractive strategy for HIV gene therapy.

Materials and Methods

Vector design and viral production

The GALV-enveloped gamma retroviral vector MT-MFR-LP2 was generated as previously described [6]. MT-MFR-PL2 expresses a truncated form of the human low affinity nerve growth factor gene (ΔLNGFR) [34] under the control of a functional PGK promoter and the MazF gene under control of the HIV-LTR promoter (Figure 1A). The ΔLNGFR is a surface marker that allows identification of transduced cells.

Animals

Four cynomolgus macaques (*Macaca fascicularis*, 6–7 years old), CD4T-1, CD4T-2, CD4T-3, and CD4T-4, were used in this experiment and were maintained at the Tsukuba Primate Research Center for Medical Science at the National Institute of Biomedical Innovation (NIBIO, Ibaraki, Japan). The study was conducted according to the Rules for Animal Care and the Guiding Principles for Animal Experiments Using Nonhuman Primates formulated by the Primate Society of Japan [35] and in accordance with the recommendations of the Weatherall report, "The use of non-human primates in research". The protocols for the experimental procedures were approved by the Animal Welfare and Animal Care Committee of the National Institute of Biomedical Innovation (DS18-100). All surgical and invasive clinical procedures were conducted by trained personnel under the supervision of a veterinarian in a surgical facility using aseptic techniques and comprehensive physiologic monitoring. Ketamine hydrochloride (Ketalar, 10 mg/kg; Daiichi-Sankyo, Tokyo, Japan) was used to induce anesthesia for all clinical procedures associated with the study protocol such as blood sampling, gene-modified cell administration, clinical examinations and treatment.

Ex vivo expansion of CD4+ T cells, and transduction of the MazF vector

Peripheral blood from cynomolgus macaques was collected by apheresis as previously described [36]. For the dissolution of red blood lymphocytes, collected blood was treated with ACK lysing buffer (Lonza, Walkersville, MD) and was washed twice with phosphate buffered saline (PBS). Then, CD4+ T cells were isolated using anti-CD4 conjugated magnetic beads (Dynal CD4 Positive Isolation Kit, Invitrogen, Carlsbad, CA) according to the manufacturer's instructions. Isolated CD4+ T cells were cultured at 5×10^5 cells/ml in GT-T503 (Takara Bio, Otsu, Japan) supplemented with 10% FBS (Invitrogen), 200 IU recombinant human interleukin-2 (IL-2; Chiron, Emeryville, CA), 2 mM L-glutamine (Lonza), 2.5 μg/ml Fungizone (Bristol Myers-Squibb, Woerden, The Netherlands) and activated for three days with either 5 μg/ml concanavalin A (Con A, Sigma Chemical, St. Louis, MO) for CD4T-1 or a combination of anti-CD3 clone FN-18 (Biosource, Camarillo, CA, USA) and anti-CD28 clone L293 (BD Biosciences, Franklin Lakes, NJ) monoclonal antibodies conjugated to M-450 epoxy magnetic beads (Invitrogen) at cell-to-bead ratio of 1:1 (CD4T-2 and CD4T-3). On day 3, the activated CD4+ T cells were transduced with the MazF retroviral vector MT-MFR-PL2 in the presence of RetroNectin® (Takara Bio) according to manufacturer's instructions. Transduction was repeated on day 4. CD4+ T cells were further expanded to day 7 to 9 until the total cell number reach more than 10^9. The closed system MazF-Tmac cell manufacturing was performed using gas permeable culture bags; Cultilife 215 (Takara Bio) and Cultilife Eva (Takara Bio) were used for CD4+ T cells expansion and Cultilife spin (Takara Bio) was used for transduction of the MazF retroviral vector.

Transplantation of expanded CD4+ T cells

Prior to the transplantation, each macaque was treated with busulfan (Ohara Pharmaceutical, Shiga, Japan). Busulfan has been used extensively as a preparatory regimen for allogenic hematopoietic stem cell transplantation based on its toxicity to hematopoietic stem cells. Furthermore, it has been reported that in non-human primates, hematopoiesis was significantly decreased after a single, clinically well-tolerated dose of busulfan, with slow, but almost complete, recovery over the next several months [20]. The effects of busulfan on lymphocyte engraftment, however, are not well documented. Although cyclophosphamide is widely used in immune gene therapy trials in humans for lymphocyte transplantation, there is no information available for cyclophosphamides effect on T-cell transplantation in the cynomolgus macaque. It should be noted that we have chosen busulfan for our CD4+ T cell transplantation because busulfan is shown to cause a reduction in the peripheral blood count in human trial [37], we have had success in using busulfan for cynomolgus macaque bone marrow transplantation and according to internal information, busulfan causes a reduction of the peripheral blood count in

cynomolgus macaques. Busulfan was orally administered to the macaques twice at 10 mg/kg each (CD4T-1 and CD4T-2) or 6 mg/kg each (CD4T-3) [38]. The expanded cells were harvested, washed three times with PBS, and re-suspended in PBS containing 10% autologous plasma. The collected cells were infused intravenously to monkeys at the speed of 1 ml per minute.

Flow cytometry analysis

The cell surface markers of the expanded cells and peripheral blood mononuclear cells (PBMC) were analyzed using FACSCalibur (BD Bioscience) and FACSCanto (BD Bioscience), and data analysis was performed using CellQuest software (BD Bioscience), FACSDiva software (BD Bioscience) or FlowJo software (Tree Star, Inc., Ashland, OR). The following antibodies were used for staining: anti-CD3 (SP34-2, PerCP), anti-CD4 (L200, FITC), anti-CD25 (2A3, FITC), anti-CD28 (CD28.2, PE), anti-CD95 (DX2, FITC), anti-CXCR4 (12G5, PE) and anti-integrin-β7 (FIB504, PE), which were obtained from BD Bioscience. The anti-CD49d (HP2/1, FITC) antibody was obtained from Beckman Coulter (Fullerton, CA), and the anti-CD271 (LNGFR, PE and APC) antibodies were obtained from Miltenyi Biotec GmbH (Bergisch Gladbach, Germany).

Measurement of hematological data

Two ml of blood was prepared every week. Blood samples were used to measure the white blood cell (WBC) count, red blood cell (RBC) count, hemoglobin (Hb) concentration, hematocrit values, mean corpuscular volume, mean cell hemoglobin concentration and platelet (PLT) count using a Sysmex K-4500 instrument (Toaiyouddenshi, Kobe, Japan). The concentrations of the biochemical markers in blood samples were also monitored including total proteins, albumin, blood urea nitrogen, glucose, glutamic oxaloacetic transaminase, glutamic pyruvic transaminase, alkaline phosphatase, creatine phosphokinase, lactate dehydrogenase, creatine, sodium, potassium, chlorine and C-reactive protein using an AU400 instrument (Olympus Medical Systems, Tokyo, Japan).

Quantification of gene-modified CD4+ T cells

The existence and persistence of genetically modified CD4+ T cells were monitored by measuring the proviral genome of the transgene using quantitative real-time PCR. DNA samples were extracted from 2×10^6 PBMCs using a Gentra Puregene Blood Kit (QIAGEN, Hilden, Germany). The proviral copy number of the transgene was calculated from 400 ng of genomic DNA with quantitative PCR using a Cycleave RT-PCR Core Kit (Takara Bio) and Provirus Copy Number Detection Primer Set (Takara Bio) according to the manufacturer's instructions. The reaction was performed with the Thermal Cycler Dice Real Time System (Takara Bio), and the data was analyzed using Multiplate RQ software (Takara Bio). For each run, a standard curve was generated from the pMT-MFR-PL2 plasmid, whose copy numbers were already known. Based on the standard curve, the amount of infused cells was quantified.

Detection of anti-MazF antibodies in macaque blood after transplantation of MazF-Tmac cells

To examine whether anti-MazF antibodies can be generated after the transplantation of MazF-Tmac cells, the plasma isolated from the macaques was analyzed. In order to detect anti-MazF antibodies, purified MazF protein or anti-monkey IgG (Nordic Immunological Laboratories, Tilburg, The Netherlands) was precoated onto the wells of a 96-well microplate and subsequently blocked with PBS-1% BSA. The plasma samples were isolated from the CD4T-2 at day 0, 33, 75, and 103 after transplantation and were diluted to 500,000-fold, 50,000-fold, and 10,000-fold. Cynomolgus macaque IgG purified from normal macaque plasma with Melon Gel IgG purification Kit (Thermo Fisher Scientific, Rockford, IL, USA) was used as a control for this reaction. The two-fold serial dilutions of the IgG (1 ng/ml to 64 ng/ml) and the diluted plasma samples, as described above, were separately added to each well. After an overnight incubation at 4°C, the wells were washed with PBS-1% BSA. The POD-conjugated anti-monkey IgG (Nordic Immunological Laboratories) was then added to the wells. After 4 hours of incubation at room temperature, the wells were washed three times with PBS-1% BSA followed by the addition of the substrate solution (o-Phenylenediamine, Sigma). The optical density of each well was read at 490/650 nm using a 680XR microplate reader (Bio-Rad Laboratories, Hercules, CA) after stopping the reaction with H_2SO_4 stop solution (Figure S1).

Examination of the anti-viral efficacy of MazF-Tmac cells harvested from a monkey

To examine the function of the *mazF* gene in cells harvested from a MazF-Tmac-transplanted monkey, the frozen lymphoid cells from CD4T-1 at autopsy (214 days post-infusion of MazF-Tmac cells) were recovered, CD4+ T cells were selected using a CD4+ T Cell Isolation Kit (Miltenyi Biotec), stimulated with anti-CD3/CD28 beads at a cell-to-bead ration of 1:1, and expanded in GT-T503 medium supplemented with 10% FBS, 200 IU recombinant human interleukin-2, 2 mM L-glutamine, 2.5 μg/ml Fungizone, 100 units/ml penicillin, and 100 μg/ml streptomycin. After 7 days of expansion, the genetically modified cells expressing ΔLNGFR+ were concentrated with an anti-CD271 monoclonal antibody (CD271 MicroBeads, Miltenyi Biotec) and expanded for 4 days. The cells from the CD271-negative fraction were also harvested and expanded as control non-gene modified CD4+ T cells. The expanded CD271-enriched cells and CD271-negative cells were infected with SHIV 89.6P at the MOI of 0.01 and cultured for 6 more days. Culture supernatants and cell pellets were harvested at 6 days post-infection. RNA in the culture supernatant was recovered with the QIAamp Viral RNA Mini Kit (QIAGEN) and SHIV RNA levels in the culture supernatant were determined by quantitative real-time PCR with a set of specific primers specific for the SHIV *gag* region [39]. In order to detect the Tat-dependent expression of MazF in the CD271-enriched MazF-Tmac cells harvested from the monkey, the cells were transduced with the Tat expression retroviral vector M-LTR-Tat-ZG [6] in the presence of RetroNectin® as per the manufacturer's instruction. Twenty hours after Tat transduction, the cells were harvested, counted by trypan blue exclusion assay, washed twice with PBS, and 5×10^5 cells were suspended in 50 μl of 1× SDS sample buffer. The cell samples were incubated at 95°C for 10 min, and 5 μl of each cell sample was used for western blot analysis. For gel electrophoresis of proteins, the sample solutions described above were loaded into the wells of a 4–20% Tris-Glycine gel (Atto, Tokyo, Japan). After completion of electrophoresis, the gel was transferred to a polyvinylidene fluoride (PVDF) membrane (Millipore, Billerica, MA) with papers containing transfer buffer using the semi-dry method at 60 mA (constant voltage) for 60 min. The membrane was cut in half horizontally around the 20 kDa protein band of the pre-stained protein marker (Bio-Rad Laboratories). The upper part of the membrane was used to detect the α-tubulin (50 kDa) as an internal standard, while the lower part of the membrane was used to detect MazF (12 kDa). After blocking, the membranes were then incubated overnight at 4°C in the blocking buffer (5% skim milk in PBS)

containing 1 μg/ml anti-α-tublin antibody (Cell Signaling Technology) and 1 μg/ml anti-MazF polyclonal antibody (rabbit, in-house preparation), respectively. Each membrane was washed three times and subsequently incubated at room temperature for 1 hour in 10 ml of the blocking buffer containing the 10,000-fold diluted goat anti-IgG rabbit antibody (peroxidase conjugated, Thermo Fisher Scientific). The membrane was washed five times by gentle shaking in the washing buffer at room temperature for 5 min. The membrane was soaked at room temperature for 5 min in substrate solution (SuperSignal West Femto Maximum Sensitivity Chemiluminescent Substrate, Thermo Scientific). Protein signals were detected by a CCD camera (LuminoShot 400 Jr, Takara Bio), which captures a digital image of the western blot.

Collection of lymphocyte from several organs

Several organs were collected following euthanasia of the monkeys. After thoracotomy, the right atrium was incised, and 2 L of heparinized PBS was infused into the left ventricle using an 18-gauge needle. After perfusion, several organs were collected, and lymphocytes were separated using the following method: samples of spleen, thymus, liver, bone marrow, and axillary, inguinal and mesenteric LNs were minced and filtered through a 40 μm nylon filter (BD Bioscience); lymphocyte of the small intestine were collected by the Percoll (GE Healthcare, Castle Hill, Australia) density-gradient centrifugation method as described previously [39]; and lymphocytes obtained from each organ were used for the flow cytometric analysis, and extracted DNA was used for quantification PCR.

In vivo homing analysis

CD4T-4 was used for homing analysis. Isolated CD4+ T cells were stimulated with anti-CD3/CD28 beads and cultured in GT-T503 medium supplemented with 10% FBS, 200 IU IL-2, 2 mM L-glutamine, and 2.5 μg/ml Fungizone. After 4 days of expansion, activated CD4+ T cells were divided into two culture bags (ClutiLife Eva), and 10 nM retinoic acid (Sigma) was added to one of the bags. After an additional 5 days of incubation, expanded cells with or without retinoic acid were harvested and labeled with 2 mM PKH26 (Sigma) or 5 μM CFSE (Sigma), respectively, according to the manufacturer's instructions. Thereafter, the cells were washed three times with PBS, mixed in PBS containing 10% autologous plasma and infused into the macaque. Then, CD4T-4 was euthanized at 3 days after transplantation. Lymphocytes from several organs were collected as previously described, and the distributions of labeled lymphocytes were detected by flow cytometric analysis. The specimens from several organs were fixed in buffered formaldehyde and embedded in plastic. Serial sections were made using a diamond saw. The slides were then analyzed under a fluorescence microscope to detect the distribution of the expanded cells in the distal organ specimens.

Supporting Information

Figure S1 Raw data of 490/650 nm absorbance. The raw data of the optical density of each well at 490/650 nm was read using a microplate reader 680XR (Bio-Rad Laboratories, Hercules, CA) is represented.
(PDF)

Figure S2 Photographs of histopathological analysis. Individual photographic data of histopathological analysis of CD4T-1, -2, and -3 in Table 3 is represented.
(PDF)

Acknowledgments

The authors thank the staff of Tsukuba Primate Research Center and Corporation for Production and Research of Laboratory Primates for the kind care and expert handling of the animals. The authors also thank Dr. Keith A. Reimann of Harvard Medical School and Dr. Tomoyuki Miura of Kyoto University for providing the SHIV 89.6P. The authors are also grateful to Dr. Koich Inoue of Takara Bio Inc. for his critical reading of this manuscript and Tomomi Sakuraba of Takara Bio Inc. for conducting the quantitative PCR assay.

Author Contributions

Conceived and designed the experiments: HC NS YY KT JM IK. Performed the experiments: HC NS HT HS NA. Analyzed the data: HC NS HS NA. Contributed reagents/materials/analysis tools: NS HT HS NA. Wrote the paper: HC NS.

References

1. Panel on Antiretroviral Guidelines for Adults and Adolescents. Guidelines for the use of antiretroviral agents in HIV-1-infected adults and adolescents. Department of Health and Human Services. December 1, 2009; 1–161. http://www.aidsinfo.nih.gov/ContentFiles/AdultandAdolescentGL.pdf. Accessed September 16, 2010.
2. Sarver N, Rossi J (1993) Gene therapy: a bold direction for HIV-1 treatment. AIDS Res Hum Retroviruses 9: 483–487.
3. Dropulic B, Jeang KT (1994) Gene therapy for human immunodeficiency virus infection: genetic antiviral strategies and targets for intervention. Hum Gene Ther 5: 927–939.
4. Dropulic B, June CH (2006) Gene-based immunotherapy for human immunodeficiency virus infection and acquired immunodeficiency syndrome. Hum Gene Ther 17: 577–588.
5. Rossi JJ, June CH, Kohn DB (2007) Genetic therapies against HIV. Nat Biotechnol 25: 1444–1454.
6. Chono H, Matsumoto K, Tsuda H, Saito N, Lee K, et al. (2011) Acquisition of HIV-1 Resistance in T Lymphocytes Using an ACA-specific *E. coli* mRNA interferase. Hum Gene Ther 22: 1–9.
7. Onlamoon N, Hudson K, Bryan P, Mayne AE, Bonyhadi M, et al. (2006) Optimization of *in vitro* expansion of macaque CD4 T cells using anti-CD3 and co-stimulation for autotransfusion therapy. J Med Primatol 35: 178–193.
8. Onlamoon N, Plagman N, Rogers KA, Mayne AE, Bostik P, et al. (2007) Anti-CD3/28 mediated expansion of macaque CD4+ T cells is polyclonal and provides extended survival after adoptive transfer. J Med Primatol 36: 206–218.
9. Pitcher CJ, Hagen SI, Walker JM, Lum R, Mitchell BL, et al. (2002) Development and homeostasis of T cell memory in rhesus macaque. J Immunol 168: 29–43.
10. Klebanoff CA, Gattinoni L, Torabi-Parizi P, Kerstann K, Cardones AR, et al. (2005) Central memory self/tumor-reactive CD8+ T cells confer superior antitumor immunity compared with effector memory T cells. Proc Natl Acad Sci U S A 102: 9571–9576.
11. Reimann KA, Li JT, Voss G, Lekutis C, Tenner-Racz K, et al. (1996) An env gene derived from a primary human immunodeficiency virus type 1 isolate confers high in vivo replicative capacity to a chimeric simian/human immunodeficiency virus in rhesus monkeys. J Virol 70: 3198–3206.
12. Engelberg-Kulka H, Hazan R, Amitai S (2005) *mazEF*: a chromosomal toxin-antitoxin module that triggers programmed cell death in bacteria. J Cell Sci 118: 4327–4332.
13. Zhang Y, Zhang J, Hoeflich KP, Ikura M, Qing G, et al. (2003) MazF cleaves cellular mRNAs specifically at ACA to block protein synthesis in *Escherichia coli*. Mol Cell 12: 913–923.
14. Suzuki M, Zhang J, Liu M, Woychik NA, Inouye M (2005) Single protein production in living cells facilitated by an mRNA interferase. Mol Cell 18: 253–261.
15. Baik S, Inoue K, Ouyang M, Inouye M (2009) Significant bias against the ACA triplet in the tmRNA sequence of *Escherichia coli* K-12. J Bacteriol 191: 6157–6166.
16. Shimazu T, Degenhardt K, Nur-E-Kamal A, Zhang J, Yoshida T, et al. (2007) NBK/BIK antagonizes MCL-1 and BCL-XL and activates BAK-mediated apoptosis in response to protein synthesis inhibition. Genes Dev 21: 929–941.
17. Levine BL, Humeau LM, Boyer J, MacGregor RR, Rebello T, et al. (2006) Gene transfer in humans using a conditionally replicating lentiviral vector. Proc Natl Acad Sci U S A 103: 17372–17377.
18. Ranga U, Woffendin C, Verma S, Xu L, June CH, et al. (1998) Enhanced T cell engraftment after retroviral delivery of an antiviral gene in HIV-infected individuals. Proc Natl Acad Sci U S A 95: 1201–1206.

19. van Lunzen J, Glaunsinger T, Stahmer I, von Baehr V, Baum C, et al. (2007) Transfer of autologous gene-modified T cells in HIV-infected patients with advanced immunodeficiency and drug-resistant virus. Mol Ther 15: 1024–1033.
20. Kuramoto K, Follman D, Hematti P, Sellers S, Laukkanen MO, et al. (2004) The impact of low-dose busulfan on clonal dynamics in nonhuman primates. Blood 104: 1273–1280.
21. Brenchley JM, Schacker TW, Ruff LE, Price DA, Taylor JH, et al. (2004) CD4+ T cell depletion during all stages of HIV disease occurs predominantly in the gastrointestinal tract. J Exp Med 200: 749–759.
22. Guadalupe M, Reay E, Sankaran S, Prindiville T, Flamm J, et al. (2003) Severe CD4+ T-cell depletion in gut lymphoid tissue during primary human immunodeficiency virus type 1 infection and substantial delay in restoration following highly active antiretroviral therapy. J Virol 77: 11708–11717.
23. Mehandru S, Poles MA, Tenner-Racz K, Horowitz A, Hurley A, et al. (2004) Primary HIV-1 infection is associated with preferential depletion of CD4+ T lymphocytes from effector sites in the gastrointestinal tract. J Exp Med 200: 761–770.
24. Mattapallil JJ, Douek DC, Hill B, Nishimura Y, Martin M, et al. (2005) Massive infection and loss of memory CD4+ T cells in multiple tissues during acute SIV infection. Nature 434: 1093–1097.
25. Li Q, Duan L, Estes JD, Ma ZM, Rourke T, et al. (2005) Peak SIV replication in resting memory CD4+ T cells depletes gut lamina propria CD4+ T cells. Nature 434: 1148–1152.
26. Picker LJ, Hagen SI, Lum R, Reed-Inderbitzin EF, Daly LM, et al. (2004) Insufficient production and tissue delivery of CD4+ memory T cells in rapidly progressive simian immunodeficiency virus infection. J Exp Med 200: 1299–314.
27. Brenchley JM, Price DA, Schacker TW, Asher TE, Silvestri G, et al. (2006) Microbial translocation is a cause of systemic immune activation in chronic HIV infection. Nat Med 12: 1365–1371.
28. Estes JD, Harris LD, Klatt NR, Tabb B, Pittaluga S, et al. (2010) Damaged intestinal epithelial integrity linked to microbial translocation in pathogenic simian immunodeficiency virus infections. PLoS Pathog 2010 Aug 19;6(8). pii: e1001052. PubMed PMID: 20808901.
29. Guadalupe M, Sankaran S, George MD, Reay E, Verhoeven D, et al. (2006) Viral suppression and immune restoration in the gastrointestinal mucosa of human immunodeficiency virus type 1-infected patients initiating therapy during primary or chronic infection. J Virol 80: 8236–8247.
30. von Andrian UH, Mackay CR (2000) T-cell function and migration. Two sides of the same coin. N Engl J Med 343: 1020–1034.
31. Wagner N, Löhler J, Kunkel EJ, Ley K, Leung E, et al. (1996) Critical role for beta7 integrins in formation of the gut-associated lymphoid tissue. Nature 382: 366–370.
32. Iwata M, Hirakiyama A, Eshima Y, Kagechika H, Kato C, et al. (2004) Retinoic acid imprints gut-homing specificity on T cells. Immunity 21: 527–538.
33. Arthos J, Cicala C, Martinelli E, Macleod K, Van Ryk D, et al. (2008) HIV-1 envelope protein binds to and signals through integrin alpha4beta7, the gut mucosal homing receptor for peripheral T cells. Nat Immunol 9: 301–309.
34. Verzeletti S, Bonini C, Marktel S, Nobili N, Ciceri F, et al. (1998) Herpes simplex virus thymidine kinase gene transfer for controlled graft-versus-host disease and graft-versus-leukemia: clinical follow-up and improved new vectors. Hum Gene Ther 9: 2243–2251.
35. Primate Society of Japan (1986) Guiding principles for animal experiments using nonhuman primates. Primate Res 2: 111–113.
36. Ageyama N, Kimikawa M, Eguchi K, Ono F, Shibata H, et al. (2003) Modification of the leukapheresis procedure for use in rhesus monkeys (*Macaca mulata*). J Clin Apher 18: 26–31.
37. Laurent J, Speiser DE, Appay V, Touvrey C, Vicari M, et al. (2010) Impact of 3 different short-term chemotherapy regimens on lymphocyte-depletion and reconstitution in melanoma patients. J Immunother 33: 723–734.
38. Masuda S, Ageyama N, Shibata H, Obara Y, Ikeda T, et al. (2009) Cotransplantation with MSCs improves engraftment of HSCs after autologous intra-bone marrow transplantation in nonhuman primates. Exp Hematol 37: 1250–1257.
39. Miyake A, Ibuki K, Enose Y, Suzuki H, Horiuchi R, et al. (2006) Rapid dissemination of a pathogenic simian/human immunodeficiency virus to systemic organs and active replication in lymphoid tissues following intrarectal infection. J Gen Virol 87: 1311–1320.

doi: 10.1111/j.1365-3083.2010.02416.x

Intradermal Delivery of Recombinant Vaccinia Virus Vector DIs Induces Gut-Mucosal Immunity

N. Yoshino*†, M. Kanekiyo†, Y. Hagiwara‡, T. Okamura†, K. Someya†, K. Matsuo†, Y. Ami§, S. Sato*, N. Yamamoto† & M. Honda†

*Department of Microbiology, School of Medicine, Iwate Medical University, Iwate; †AIDS Research Center, National Institute of Infectious Diseases, Tokyo; ‡Research Center for Biologicals, The Kitasato Institute, Saitama; and §Division of Experimental Animals Research, National Institute of Infectious Diseases, Tokyo, Japan

Received 15 March 2010; Accepted in revised form 29 April 2010

Correspondence to: N. Yoshino, Department of Microbiology, School of Medicine, Iwate Medical University, 19-1 Uchimaru, Morioka, Iwate 020-8505, Japan. E-mail: nyoshino@iwate-med.ac.jp

Abstract

Antigen-specific mucosal immunity is generally induced by the stimulation of inductive mucosal sites. In this study, we found that the replication-deficient vaccinia virus vector, DIs, generates antigen-specific mucosal immunity and systemic responses. Following intradermal injection of recombinant DIs expressing simian immunodeficiency virus *gag* (rDIsSIV*gag*), we observed increased levels of SIV p27-specific IgA and IgG antibodies in faecal extracts and plasma samples, and antibody-forming cells in the intestinal mucosa and spleen of C57BL/6 mice. Antibodies against p27 were not detected in nasal washes, saliva, and vaginal washes. The enhanced mucosal and systemic immunity persisted for 1 year of observation. Induction of Gag-specific IFN-γ spot-forming $CD8^+$ T cells in the spleen, small intestinal intraepithelial lymphocytes, and submandibular lymph nodes was observed in the intradermally injected mice. Heat-inactivated rDIsSIV*gag* rarely induced antigen-specific humoral and T-helper immunity. Moreover, rDIsSIV*gag* was detected in MHC class II IA antigen-positive (IA^+) cells at the injection site. Consequently, intradermal delivery of rDIs effectively induces antigen-specific humoral and cellular immunity in gut-mucosal tissues of mice. Our data suggest that intradermal injection of an rDIs vaccine may be useful against mucosally transmitted pathogens.

Introduction

As most infectious agents, including human immunodeficiency virus (HIV), are often transmitted via mucosal surfaces, a mucosal-inductive vaccine capable of eliciting protective immunity in mucosal tissues and external secretions would act as the first line of defence at the site of initial invasion. For inducting preventive immunity to HIV, a vaccine must induce anti-HIV neutralizing antibodies (Ab) and/or cytotoxic T lymphocytes against HIV-infected cells in the mucosal and submucosal areas [1]. Parenterally immunized vaccines generally do not enhance the levels of secretory IgA Ab production in external secretions and are less able to induce the mucosal immune responses needed to prevent infection at the site of initial contact between the host and the infectious agent [2–4].

Poxvirus vectors are among the most heavily exploited for vaccine development. Their use is largely attributable to the overwhelming success of the vaccinia virus vaccine in eradicating smallpox. Because of concerns regarding the use of a replicating vector in immunocompromised individuals, non-replicating poxvirus vectors, such as the modified vaccinia virus Ankara (MVA) [5], are an area of interest for extensive development. The replication-deficient vaccinia virus, DIs, is a candidate viral vector; and it is a safe and highly attenuated mutant of the vaccinia virus [6–9]. When recombinant DIs (rDIs) encoding foreign antigens (Ag) was intravenously [9, 10], intramuscularly [11, 12], subcutaneously [13], or intradermally [14] injected, Ag-specific systemic immunity was induced in mice and non-human primates.

Activation of the inductive sites is of paramount importance to induce Ag-specific mucosal immunity. Intradermal and intramuscular injection of a DNA vaccine generates solely systemic but rarely mucosal responses [15, 16]. The potential importance of specific mucosal immunity in the protection against mucosally transmitted pathogens is beginning to emerge from many investigations. We had previously demonstrated that intranasal or intragastrical administration of rDIs encoding full-length simian immunodeficiency virus *gag*

(rDIsSIV*gag*) could induce Gag-specific cytotoxic T lymphocytes and p27-specific Ab in both the systemic sites and the mucosal sites of mice [17].

In recent clinical studies, the smallpox vaccine was administered by skin scarification, subcutaneous, intramuscular, or intradermal vaccination [18–20]. Immunization of the mice with MVA by skin scarification protected the mice against intranasal challenge with pathogenic Western Reserve vaccinia virus in mice, but intramuscular immunization was ineffective [21]. Subcutaneous injection of rDIs was inefficient to induce Ag-specific mucosal IgA Ab responses whereas high IgG Ab responses were induced in the plasma [13]. DIs vaccines are typically parenterally injected; however, mucosal immunity has not been tested in parenterally injected animals. An advantage of intradermal injection is that all the materials for intradermal injection are readily available and accessible to clinicians. Therefore, we studied whether intradermal injection of rDIs induces mucosal immunity. Here, we describe the enhanced induction of humoral and cellular immunity in the mucosal tissues of mice injected intradermally with the DIs vector.

Materials and methods

Recombinant vaccinia virus vectors. The production and preparation of rDIsSIV*gag* and rDIs expressing LacZ (rDIsLacZ) as a control vector have been described in detail previously [9, 11]. To prepare heat-inactivated rDIsSIV*gag*, 10^5 PFU of rDIsSIV*gag* was incubated at 56 °C for 30 min. The PFU of heat-inactivated rDIsSIV*gag* was confirmed as < 2 by a chicken embryo fibroblast culture [22, 23]. These vectors were stored at −80 °C until used.

Mice. Five-week-old C57BL/6N mice were purchased from Charles River Japan, Inc. (Yokohama, Japan). The mice were acclimated to the experimental animal facility for more than 1 week before being used in the experiments. They were maintained in the facility under pathogen-free conditions. All experimental procedures were performed in accordance with the guidelines established by the National Institute of Infectious Diseases, Japan. The study was conducted in a biosafety level 2 facility under the approval of an institutional committee for biosafety and in accordance with the requirements of the World Health Organization. In cases of specification, systemic vaccination against pathogenic viruses or bacteria induced mucosal secretory IgA Ab responses in individuals who had previously been exposed to its pathogen by the mucosal route [24–26]. That, of course, is negated here because we used naive mice in this study, and p27-specific Ab were not detected in the plasma and faecal extracts of the mice before immunization.

Immunization. The mice were injected intradermally at the interscapular region thrice at weekly intervals in two contiguous sites with a 25-μl aliquot of PBS containing 10^5 PFU per 50 μl of rDIsSIV*gag* or rDIsLacZ. The mice were extensively washed with warm water, blot-dried, and then washed and dried again to avoid acquiring small amounts of injected rDIs through their normal grooming activity. To compare with the mucosal immunization, the mice were immunized with 10^5 PFU of rDIsSIV*gag* by the nasal route thrice at weekly intervals according to previously described methods [17].

Sample collection and preparation of single-cell suspensions. After immunization, blood and mucosal secretions (faecal extracts, nasal washes, saliva, and vaginal washes) were collected by using methods described elsewhere [27–30]. Vaginal washes were pooled from four mice for each experiment [30]. The collected samples were stored at −80 °C until used. Single-cell suspensions were obtained from the spleen, mesenteric lymph nodes (MLN), submandibular lymph nodes (SMLN), axillary lymph nodes (ALN), small intestinal lamina propria (i-LP), and small intestinal intraepithelial lymphocytes (IEL) as previously described [29].

Analysis of IFN-γ production of SIV Gag peptide-specific $CD8^+$ T cells. To detect Gag-specific cellular immunity, $CD8^+$ T cells in the spleen, IEL, and SMLN of mice were cultured with or without overlapping Gag peptide. The methods of $CD8^+$ T cell enrichment and Gag-specific IFN-γ spot-forming cells (SFC) assessed by enzyme-linked immunosorbent spot (ELISPOT) assay were as described previously [17]. The number of Gag-specific IFN-γ SFC was calculated by subtracting the results of the control culture (i.e. without Gag peptide stimulation) from those of the peptide-stimulated culture, because non-specific activated $CD8^+$ T cells produced IFN-γ.

Detection of SIV p27-specific Ab production by ELISA and enumeration of p27-specific Ab-forming cells by ELISPOT assay. Titres of p27-specific Ab in the plasma and mucosal secretions were determined by an endpoint enzyme-linked immunosorbent assay (ELISA). The endpoint titres were expressed as the last dilution that gave an optical density at 450 nm (OD_{450}) of ≥ 0.1 OD units above the OD_{450} of the negative controls [17]. SIV p27-specific IgA, IgG, and IgM Ab-forming cells (AFC) in the spleen, i-LP, and MLN of mice were determined by ELISPOT assay. SIV p27-specific AFC were quantitated with the aid of a stereomicroscope [17].

Cytokine production of SIV Gag peptide-specific $CD4^+$ T cells. Overlapping Gag peptide-specific helper immunity of $CD4^+$ T cells in the spleen of mice was measured by ELISA. The methods of $CD4^+$ T-cell purification and culture conditions were as described previously [17]. The levels of IFN-γ, IL-4, and IL-10 were measured by ELISA kit (eBioscience, San Diego, CA, USA). The levels of Gag-specific IFN-γ, IL-4, and IL-10 in the culture supernatants were calculated by subtracting the results of the

control cultures from those of the Gag peptide-stimulated cultures.

Isolation of IA$^+$ cells in the skin. Twenty-four hours after the intradermal injection of 10^7 PFU rDIsSIV*gag*, the mice were shaved at the vaccinal locus with a razor. The skin was then removed and cut to approximately 1×1 cm^2 of the vaccinal locus. MHC class II IA antigen-positive (IA$^+$) cells were isolated from the skin by enzymatic dissociation protocols [31]. The epidermal cells were incubated with anti-I-A^b monoclonal Ab (AF6-120.1; Becton Dickinson, San José, CA, USA). IA$^+$ cells were isolated by auto MACS (Miltenyi Biotec GmbH, Bergisch Gladbach, Germany). The purified fractions included > 97% IA$^+$ cells.

Preparation of DNA samples and amplification of SIV gag gene by nested PCR. For determining the distribution of rDIsSIV*gag*, a nested PCR was used to amplify a fragment of the *gag* gene segment. DNA samples were prepared from the skin, skin IA$^+$ cells, ALN, SMLN, Peyer's patches (PP) and spleen. The preparation, amplification methods, and primer sequences are described elsewhere [17, 32]. The lowest concentration of plasmid SIV DNA detectable with this PCR method in the first amplification with an outer *gag* primer pair was 10^3 copies. Upon further amplification with nested/internal *gag* primers, a single copy of plasmid DNA could be routinely detected [32].

Statistical analysis. Normally distributed variables were compared by the two-tailed Student's *t*-test, and the results are expressed as the mean ± the standard deviation (SD). Non-normally distributed variables were compared by the two-tailed Mann–Whitney *U* test, and the results are expressed as the median and the interquartile range (IQR). A P value < 0.05 was considered significant.

Results

Cellular and humoral immunity by intradermal injection of rDIs

The first step was to assess whether intradermal injection of rDIsSIV*gag* induces Gag-specific IFN-γ-producing CD8$^+$ T cells in mucosal and systemic tissues. Although the BCG vector itself non-specifically enhances the levels of some cytokines [33], the DIs empty vector and rDIsLacZ scarcely stimulated IFN-γ-production, and the number of IFN-γ SFC per 10^6 cells was less than 32 in intradermally injected mice [14] and intramuscularly injected non-human primates [12] in our previous studies. Moreover, the calculated number of Gag-specific IFN-γ SFC from naive mice was < 15 per 10^6 CD8$^+$ T cells. A calculated number of SFC above 15 was considered positive. The number of Gag-specific IFN-γ SFC in the spleen in the intradermal injection group was significantly higher than that of the mice immunized intranasally with the same dose of rDIsSIV*gag*. Conversely, the number of IFN-γ SFC in the IEL of the mice injected intradermally was significantly lower than that of the intranasally immunized mice. There was no significant difference in the SMLN between the intradermally injected group and the intranasally immunized group (Fig. 1). Gag-specific IFN-γ-producing CD8$^+$ T cells were apparent in both mucosal and systemic tissues in the intradermally injected mice.

Ag-specific Ab, especially secretory IgA Ab in mucosal secretions, have been shown to be of central importance for host defence [1, 34]. We assessed the Ab response to p27 in the plasma and faecal extracts of immunized mice at 1 week after the last immunization. Intradermal injection of rDIsSIV*gag* induced p27-specific IgG Ab in the plasma, and p27-specific IgA Ab in the faecal extracts in six of the eight (75%) mice at 1 week after the last intradermal injection. Remarkably, the titres of p27-specific IgA Ab in the faecal extracts of mice immunized intradermally or intranasally with rDIsSIV*gag* were roughly equivalent (Fig. 2). However, p27-specific IgA Ab were not detected in the nasal washes, saliva, and vaginal washes of intradermally injected mice (data not shown). The p27-specific IgG and IgA Ab titres in the plasma and faecal extracts from the mice intradermally injected with rDIsLacZ (negative controls) were less than the detection limit on endpoint ELISA among (data not shown).

Intragastric immunization with rDIsSIV*gag* has been reported to induce p27-specific IgA Ab in the faecal

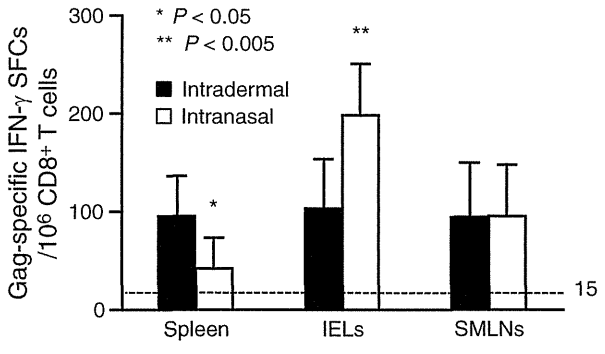

Figure 1 Intradermal injection of rDIsSIV*gag* induced SIV Gag-specific IFN-γ-secreted CD8$^+$ T cells in both mucosal tissues and systemic tissue. CD8$^+$ T cells were isolated one week after the last injection from the spleen, IEL, and SMLN of the mice injected intradermally (closed column) or intranasally (open column) with 10^5 PFU of rDIsSIV*gag*. IFN-γ production was assessed by ELISPOT assay. The number of Gag-specific IFN-γ SFC was calculated by subtracting the results of the control culture from those of the peptide-stimulated culture. The data are shown as the mean number of SFC per 10^6 CD8$^+$ T cells + SD for eight mice in each group and are representative of two separate experiments. Each group was compared by two-tailed Student's *t*-test. Significant differences between the intranasal group and the intradermal group are indicated with an asterisk (*P < 0.05, **P < 0.005).

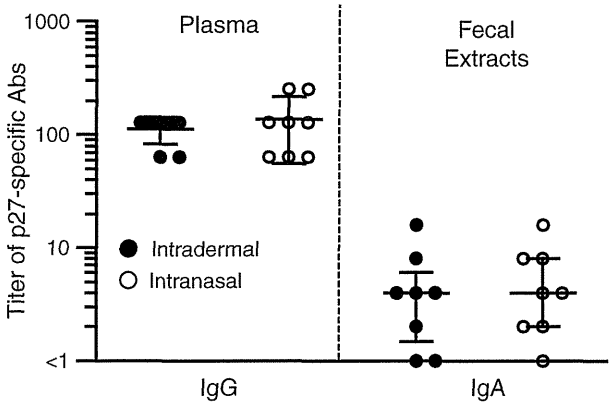

Figure 2 Intradermal injection of rDIsSIV*gag* induced SIV p27-specific Ab in the plasma. The mice were killed one week after the last immunization. The titres of p27-specific IgG Ab in the plasma and IgA Ab in the faecal extracts of the mice injected intradermally or intranasally with 10^5 PFU of rDIsSIV*gag* were determined by ELISA. Each dot represents an individual mouse. The horizontal and vertical bars indicate the mean ± SD for eight mice in each experimental group and are representative of two separate experiments. The titre of the IgG Ab in the plasma of each group was compared by two-tailed Student's *t*-test, and the titre of the IgA Ab in the faecal extracts of each group was compared by the two-tailed Mann–Whitney *U* test.

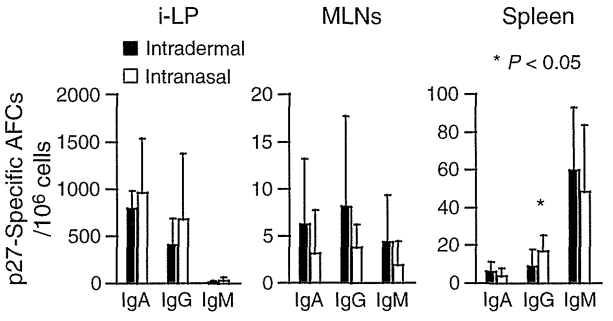

Figure 3 Intradermal injection of rDIsSIV*gag* induced SIV p27-specific AFC in the mucosal and systemic tissues. The mice were killed one week after the last immunization. The levels of p27-specific IgA, IgG, and IgM AFC in the i-LP, MLN, and spleen of the mice injected intradermally (closed column) or intranasally (open column) with 10^5 PFU of rDIsSIV*gag* were determined by ELISPOT assay. The data are shown as the mean number of AFC per 10^6 cells + SD for eight mice and representative of two separate experiments. The number of AFCs in the tissues of each group was compared by two-tailed Student's *t*-test.

extracts of mice at 1 week after the last immunization [17]. IgA Ab against p27 were detected in four of the eight (50%) mice that were intragastrically administered 10^5 PFU of rDIsSIV*gag*, and the range of the IgA Ab titre was < 2–32 [17]. The statistical significance of the differences among the three groups was assessed using Kruskal–Wallis test (P = 0.6818). We found that intradermal injection of rDIsSIV*gag* induced p27-specific IgA Ab in the faecal extracts at similar titres as observed after intranasal and intragastric immunization among mice receiving the same dose.

We also assessed the number of p27-specific AFC induced in the i-LP, MLN, and spleen after intradermal injection of rDIsSIV*gag*. We found clear evidence of p27-specific IgA AFC in the i-LP of the mice injected intradermally with rDIsSIV*gag*. The AFC were detected in the i-LP and MLN of mice intradermally injected with rDIsSIV*gag*, with similar levels of the IgA AFC observed for intranasal group receiving the same dose. Only the number of p27-specific IgG AFC in the spleen significantly differed among the intradermal and intranasal groups (Fig. 3). No p27-specific AFC were detected in the tested tissues of the mice intradermally injected with rDIsLacZ (data not shown).

Assessment of long-lasting p27-specific Ab production by intradermal rDIs injection

As long-lived memory B and T cells are responsible for the long-lasting immunity elicited by smallpox vaccination in humans [35, 36], we investigated the duration of p27-specific long-lasting humoral immune responses in the systemic and mucosal sites of the mice intradermally injected with rDIsSIV*gag*. 1 week after the last injection, titres of p27-specific IgG Ab were detected in the plasma and peaked at 17–25 weeks. Thereafter, the Ab titres were maintained in the plasma until 49 weeks of testing (~ 1 year) without further boosting (Fig. 4A). Interestingly, p27-specific IgM Ab were observed in the plasma of these mice throughout the 1-year period (Fig. 4A). The levels of p27-specific IgA Ab did not correlate with those of IgG and IgM Ab; increases in p27-specific IgA Ab titres were observed until 11 weeks after the last injection. After peaking, IgA Ab were barely detected in the plasma for 1 year, and the mean titre of IgA Ab in the intradermally injected mice declined to a value between 22 and 56 (Fig. 4A).

After that p27-specific IgA Ab were detected in the faecal extracts from six of eight mice at 1 week; these Ab were detected in the faecal extracts of all the mice at 11 and 25 weeks. Moreover, the Ab in the faecal extracts were detected after approximately 1 year in four of eight (50%) mice (Fig. 4B). Although p27-specific IgG Ab in the faecal extracts were also detected at 1 week after the last injection, they were not observed at 25 and 49 weeks (Fig. 4B).

Intradermal injection of heat-inactivated rDIs

Mice were intradermally injected with live or heat-inactivated rDIsSIV*gag* and killed at 1 week after the last injection. The mean number of p27-specific IgA AFC in the i-LP of the mice intradermally injected with live and heat-inactivated rDIsSIV*gag* was 788.4 and 12.5 AFC per 10^6 cells, respectively. SIV p27-specific AFC in all the assessed tissues were scarcely induced in the mice injected

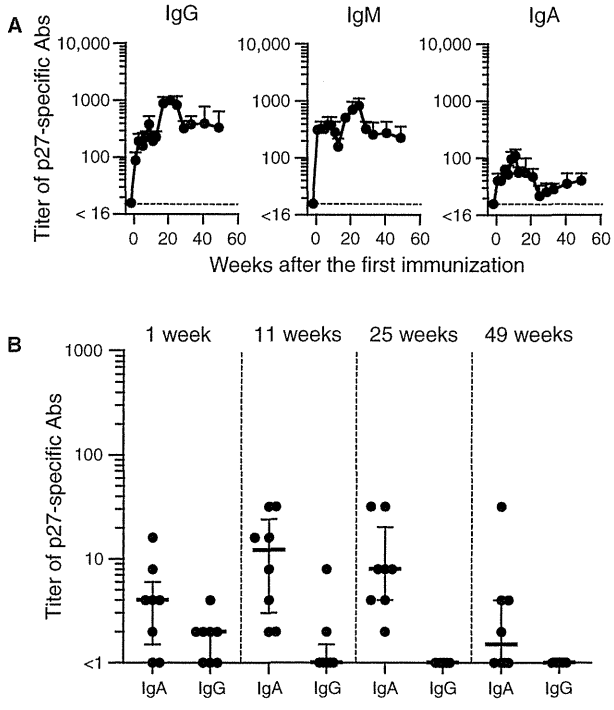

Figure 4 Intradermal injection of rDIsSIV*gag* induced long-lasting humoral immune responses. The mice were intradermally injected with 10^5 PFU of rDIsSIV*gag*. Plasma p27-specific IgG, IgM, and IgA Ab (A) and IgA and IgG Ab in faecal extracts (B) were determined by an end-point ELISA. Plasma Ab are shown as the mean titres + SD for eight mice. Faecal pellets were collected at 1, 11, 25, and 49 weeks after the last injection. Each dot in (B) represents an individual mouse. The horizontal and vertical bars indicate the median and IQR. The data are representative of two separate experiments.

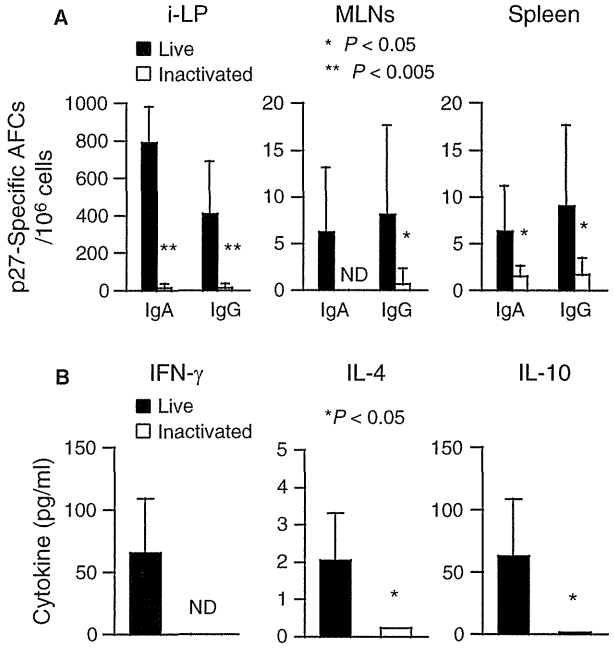

Figure 5 Intradermal injection of heat-inactivated rDIsSIV*gag* did not induce SIV Gag-specific immunity. (A) The mice were intradermally injected with 10^5 PFU of rDIsSIV*gag* (closed column) and heat-inactivated rDIsSIV*gag* (open column) and were killed 1 week after the last injection. The levels of p27-specific IgA and IgG AFC in the *i*-LP, MLN, and spleen were determined by ELISPOT assay. (B) $CD4^+$ T cells were isolated from the spleen 1 week after the last injection. Culture supernatants were harvested and then analysed by ELISA for the production of IFN-γ, IL-4, and IL-10. The data are shown as the mean number of AFC per 10^6 cells or the mean concentration of cytokines + SD for eight mice in each experimental group and are representative of two separate experiments. Each group was compared by two-tailed Student's *t*-test. Significant differences between the live rDIs group and the heat-inactivated rDIs group are indicated with an asterisk (*$P < 0.05$, **$P < 0.005$). ND: not detected.

with inactivated rDIsSIV*gag* (Fig. 5A). Furthermore, we assessed the Gag-specific T helper (Th1)-type and Th2-type responses. Intradermal injection of live rDIsSIV*gag* resulted in effective helper T-cell responses. In contrast, Gag-specific Th2-type responses (IL-4 and IL-10) in the mice injected with inactivated rDIsSIV*gag* were significantly lower than those in the mice injected with live rDIsSIV*gag*. Further, Th1-type responses (IFN-γ) were not detected in the mice injected with inactivated rDIsSIV*gag* (Fig. 5B).

Distribution of rDIs following intradermal injection

The skin is the ideal site for vaccination because of the presence of Ag-presenting cells such as the Langerhans cells (LC) and dermal dendritic cells (DC) expressing IA MHC class II antigen [37]. When the mice were killed at 1 day after intradermal injection, the *gag* gene was detected in the skin around the injection site. The gene was also detected in the IA^+ cells isolated from the skin injected with rDIsSIV*gag*. In the lymphoid tissues, the *gag* gene was detected in the ALN and SMLN of six of the eight (75%) mice. However, the gene was not detected in the spleen and PP of mice by nested PCR at this time point (Fig. 6).

Discussion

We have demonstrated here that intradermal injection of rDIs could induce Ag-specific immune responses detectable in both the mucosal tissues and systemic tissue of mice. The longevity and stability of immune memory is one of the key factors in vaccine development. In this study, p27-specific IgA Ab in the faecal extracts and plasma IgG Ab immune responses persisted for 1 year of observation. Moreover, IgM Ab against p27 in the plasma were detected throughout the period of Ab monitoring. However, the mechanism governing prolonged p27-specific Ab induction including the IgM subclass has yet to be elucidated. We theorize that sufficient quantities of Gag were continuously produced in the mice to reactivate IgM Ab production in the

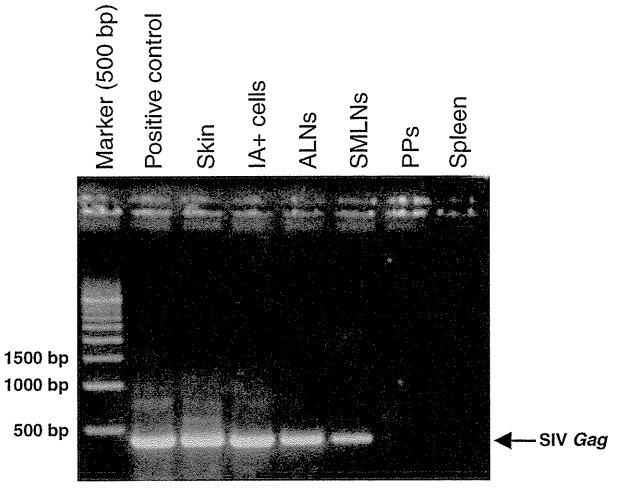

Figure 6 Distribution of rDIsSIV*gag* in the intradermally injected mice. The mice were intradermally injected with 10^7 PFU of rDIsSIV*gag* and killed 1 day after injection. The *gag* gene was assessed in the skin, IA^+ cells, ALN, SMLN, PP, and spleen by nested PCR. The gene was detected in the skin and IA^+ cells of all eight mice, in the ALN and SMLN of six mice, but never in the PP and spleen. Amplification with the first-round primers resulted in a band at 613 bp and amplification with the nested primers resulted in a band at 405 bp.

absence of viral replication and reinfection, although we did not assess long-lasting rDIs vector persistence in the mucosal tissues.

Intradermal injection of rMVA induced Ag-specific IgA Ab in faecal extracts and lung washes [38]. It is important to consider that plasma-derived transport of dimeric or polymeric IgA Ab from the systemic circulation into the gut via hepatobiliary transport can influence the titre of IgA Ab in faecal extracts, because of a large portion of murine gut IgA Ab is derived from blood rather than mucosal production [39–41]. Our previous study had showed that intragastric immunization with rDIsSIV*gag* induced p27-specific IgA AFC in i-LP (mean number of IgA AFC, 1994 ± 317) [17]. The number of p27-specific IgA AFC in the i-LP of mice intradermally immunized rDIsSIV*gag* was significantly lower than that in the intragastric group (P = 0.0041). However, the titres of p27-specific IgA Ab in the faecal extracts of mice immunized intradermally or intragastrically with rDIs were roughly equivalent (P = 0.645). Oral immunization induces substantial Ab responses in the small intestine [42, 43]. Intranasal immunization evokes Ab responses in the upper airway mucosa and regional secretions, but not in the gut [44, 45]. Although we could not determine which mucosal tissue(s) produce large amounts of dimeric or polymeric IgA Ab against specific Ag by intradermal injection, our findings validate the notion that intradermal injection of rDIs induces a good level of Ag-specific IgA Ab in the intestinal mucosa.

In this study, the mechanism(s) underlying the induction of immune responses against foreign Ag at mucosal sites by the intradermal injection of the rDIs vector was unclear. The *gag* gene was detected in IA^+ cells isolated from skin injected with rDIsSIV*gag*; heat-inactivated rDIsSIV*gag* rarely induces Ag-specific immune responses. These findings may be key in elucidating the above-mentioned mechanism of immune response induction. Further, intradermal passive transfer of rDIsSIV*gag*-infected IA^+ cells induced intestinal mucosal immunity against p27 (unpublished data). These findings suggest that IA^+ LC and/or dermal DC may be one of the responsible cells for the induction of gut-mucosal immunity, and immune induction may require an activated molecular viral life cycle of rDIs.

Intradermal and intranasal immunization with rDIsSIV*gag* induced Gag-specific IFN-γ SFC in SMLN. SMLN contribute to the mucosal immune responses [46, 47] and are one of the secondary lymphoid tissues for mucosal immunity on intranasal immunization [48]. The *gag* gene was detected in the SMLN; however, it remains to be confirmed whether LC, DC, and/or other skin immunity-associated cells [49–52] transfer the rDIsSIV*gag* into draining SMLN. In a study of transcutaneous immunization, $langerin^+$ DC in MLN were found to play a key role in the mutual relationship between the skin immune system and the gut immune system [53]. The *gag* gene was also detected in the ALN. The ALN might be one of the regional LNs in mice injected intradermally in the interscapular region, and systemic immune responses might be activated in the ALN. To investigate the association between intradermal injection and gut mucosa, activated lymphocytes and Ag-presenting cells in the draining LNs of mice should be assessed in future studies.

In conclusion, this study has shown that intradermal delivery of a recombinant vaccinia virus vector, DIs, induces gut-mucosal immunity in mice. However, the observed titres of IgA Ab in the faecal extracts and IgG Ab in the plasma of the mice injected with rDIs alone were not very high. Further, there is no conclusive evidence whether intradermal injection of rDIs provides adequate specific immunity against mucosally transmitted pathogens at mucosal sites. Within the limitations of our study, however, we have shed light on the intradermal route of rDIs injection to induce mucosal immunity and provided an important step towards the development of an effective intradermal rDIs vaccine against mucosally transmitted agents.

Acknowledgment

This work was supported by the Human Science Foundation of Japan, and the Japanese Ministry of Health, Labor, and Welfare. A part of this work was supported by a grant from the Keiryokai Research Foundation (No. 94). The authors declare no conflict of interest.

References

1 Letvin NL. Progress and obstacles in the development of an AIDS vaccine. *Nat Rev Immunol* 2006;12:930–9.

2 Ogra PL, Karzon DT, Righthand F *et al.* Immunoglobulin response in serum and secretions after immunization with live and inactivated poliovaccine and natural infection. *N Engl J Med* 1968;279:893–900.

3 Ogra PL, Chiba Y, Beutner KR, Morag A. Vaccination by non-parenteral routes: characteristics of immune response. *Dev Biol Stand* 1976;33:19–26.

4 Kiyono H, Czerkinsky C. Consideration of mucosally induced tolerance in vaccine development. In: Kiyono H, Ogra PL, McGhee JR, eds. *Mucosal Vaccine*. San Diego: Academic Press, 1996:89–101. ISBN: 0-12-410580-7

5 Moss B. Genetically engineered poxviruses for recombinant gene expression, vaccination, and safety. *Proc Natl Acad Sci USA* 1996;93:11341–8.

6 Tagaya I, Kitamura T, Sano Y. A new mutant of dermovaccinia virus. *Nature* 1961;192:381–2.

7 Kitamura T, Kitamura Y. Interference with the growth of vaccinia virus by an attenuated mutant virus. *Jpn J Med Sci Biol* 1963;16:343–57.

8 Kitamura T, Kitamura Y, Tagaya I. Immunogenicity of an attenuated strain of vaccinia virus on rabbits and monkeys. *Nature* 1967;215:1187–8.

9 Ishii K, Ueda Y, Matsuo K *et al.* Structural analysis of vaccinia virus DIs strain: application as a new replication-deficient viral vector. *Virology* 2002;302:433–44.

10 Ami Y, Izumi Y, Matsuo K *et al.* Priming-boosting vaccination with recombinant *Mycobacterium bovis* Bacillus Calmette-Guérin and a nonreplicating vaccinia virus recombinant leads to long-lasting and effective immunity. *J Virol* 2005;79:12871–9.

11 Someya K, Xin KQ, Matsuo K *et al.* A consecutive priming-boosting vaccination of mice with simian immunodeficiency virus (SIV) *gag/pol* DNA and recombinant vaccinia virus strain DIs elicits effective anti-SIV immunity. *J Virol* 2004;78:9842–53.

12 Someya K, Ami Y, Nakasone T *et al.* Induction of positive cellular and humoral immune responses by a prime-boost vaccine encoded with simian immunodeficiency virus *gag/pol*. *J Immunol* 2006;176:1784–95.

13 Ishii K, Hasegawa H, Nagata N *et al.* Induction of protective immunity against severe acute respiratory syndrome coronavirus (SARS-CoV) infection using highly attenuated recombinant vaccinia virus DIs. *Virology* 2006;351:368–80.

14 Okamura T, Someya K, Matsuo K, Hasegawa A, Yamamoto N, Honda M. Recombinant vaccinia DIs expressing simian immunodeficiency virus gag and pol in mammalian cells induces efficient cellular immunity as a safe immunodeficiency virus vaccine candidate. *Microbiol Immunol* 2006;50:989–1000.

15 McCluskie MJ, Davis HL. Novel strategies using DNA for the induction of mucosal immunity. *Crit Rev Immunol* 1999;19:303–29.

16 Stevceva L, Abimiku AG, Franchini G. Targeting the mucosa: genetically engineered vaccines and mucosal immune responses. *Genes Immun* 2000;1:308–15.

17 Yoshino N, Kanekiyo M, Hagiwara Y *et al.* Mucosal administration of completely non-replicative vaccinia virus recombinant Dairen I strain elicits effective mucosal and systemic immunity. *Scand J Immunol* 2008;68:476–83.

18 Frey SE, Newman FK, Yan L, Lottenbach KR, Belshe RB. Response to smallpox vaccine in persons immunized in the distant past. *JAMA* 2003;289:3295–9.

19 Greenberg RN, Kennedy JS, Clanton DJ *et al.* Safety and immunogenicity of new cell-cultured smallpox vaccine compared with calf-lymph derived vaccine: a blind, single-centre, randomised controlled trial. *Lancet* 2005;365:398–409.

20 Kennedy JS, Greenberg RN. IMVAMUNE: modified vaccinia Ankara strain as an attenuated smallpox vaccine. *Expert Rev Vaccines* 2009;8:13–24.

21 Liu L, Zhong Q, Tian T, Dubin K, Athale SK, Kupper TS. Epidermal injury and infection during poxvirus immunization is crucial for the generation of highly protective T cell-mediated immunity. *Nat Med* 2010;16:224–7.

22 Tagaya I, Amano H, Yuasa T. Improved plaque assay of a mutant of vaccinia virus, strain DIs, in chick embryo cell cultures. *Jpn J Med Sci Biol* 1974;27:245–7.

23 Morita M, Aoyama Y, Arita M *et al.* Comparative studies of several vaccinia virus strains by intrathalamic inoculation into cynomolgus monkeys. *Arch Virol* 1977;53:197–208.

24 Svennerholm AM, Holmgren J, Hanson LA, Lindblad BS, Quereshi F, Rahimtoola RJ. Boosting of secretory IgA antibody responses in man by parenteral cholera vaccination. *Scand J Immunol* 1977;6:1345–9.

25 Svennerholm AM, Hanson LA, Holmgren J, Lindblad BS, Nilsson B, Quereshi F. Different secretory immunoglobulin A antibody responses to cholera vaccination in Swedish and Pakistani women. *Infect Immun* 1980;30:427–30.

26 Svennerholm AM, Hanson LA, Holmgren J *et al.* Antibody responses to live and killed poliovirus vaccines in the milk of Pakistani and Swedish women. *J Infect Dis* 1981;143:707–11.

27 Wu HY, Russell MW. Induction of mucosal immunity by intranasal application of a streptococcal surface protein antigen with the cholera toxin B subunit. *Infect Immun* 1993;61:314–22.

28 Tamura S, Miyata K, Matsuo K *et al.* Acceleration of influenza virus clearance by Th1 cells in the nasal site of mice immunized intranasally with adjuvant-combined recombinant nucleoprotein. *J Immunol* 1996;156:3892–900.

29 Moldoveanu Z, Fujihashi K. Collection and processing of external secretions and tissues of mouse origin. In: Mestecky J, Lamm ME, McGhee JR, Bienenstock J, Mayer L, Strober W, eds. *Mucosal Immunology*, 3rd edn. San Diego: Academic Press, 2005:1841–52.

30 Yoshino N, Fujihashi K, Hagiwara Y *et al.* Co-administration of cholera toxin and apple polyphenol extract as a novel and safe mucosal adjuvant strategy. *Vaccine* 2009;27:4808–17.

31 Schuler G, Steinman RM. Murine epidermal Langerhans cells mature into potent immunostimulatory dendritic cells *in vitro*. *J Exp Med* 1985;161:526–46.

32 Unger RE, Marthas ML, Lackner AA *et al.* Detection of simian immunodeficiency virus DNA in macrophages from infected rhesus macaques. *J Med Primatol* 1992;21:74–81.

33 Pelizon AC, Martins DR, Zorzella-Pezavento SFG *et al.* Neonatal BCG immunization followed by DNAhsp65 boosters: highly immunogenic but not protective against tuberculosis – a paradoxical effect of the vector? *Scand J Immunol* 2010;71:63–9.

34 Brandtzaeg P. Mucosal immunity: induction, dissemination, and effector functions. *Scand J Immunol* 2009;70:505–15.

35 Crotty S, Felgner P, Davies H, Glidewell J, Villarreal L, Ahmed R. Cutting edge: long-term B cell memory in humans after smallpox vaccination. *J Immunol* 2003;171:4969–73.

36 Combadiere B, Boissonnas A, Carcelain G *et al.* Distinct time effects of vaccination on long-term proliferative and IFN-γ-producing T cell memory to smallpox in humans. *J Exp Med* 2004;199:1585–93.

37 Romani N, Ratzinger G, Pfaller K *et al.* Migration of dendritic cells into lymphatics-the Langerhans cell example: routes, regulation, and relevance. *Int Rev Cytol* 2001;207:237–70.

38 Wyatt LS, Belyakov IM, Earl PL, Berzofsky JA, Moss B. Enhanced cell surface expression, immunogenicity and genetic stability result-

